

RD-A190 701

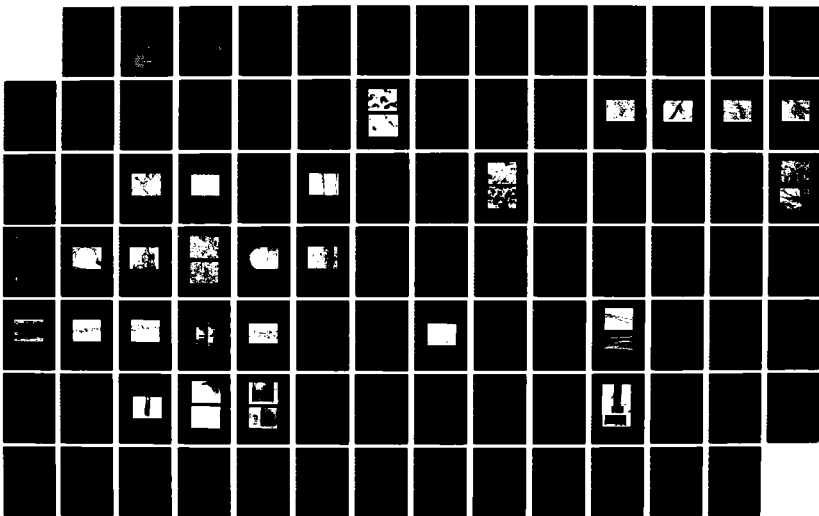
COMPOSITE CERAMIC SUPERCONDUCTING FILAMENTS FOR  
SUPERCONDUCTING CABLE(U) CERAMICS PROCESS SYSTEMS CORP  
CAMBRIDGE MA J W HALLORAN 05 JAN 87 N00014-87-C-0789

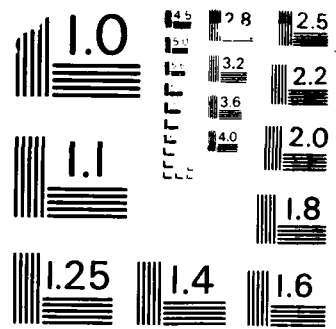
1/1

UNCLASSIFIED

F/G 9/1

NL





MICROCOPY RESOLUTION TEST CHART  
NATIONAL BUREAU OF STANDARDS-1963-A

4

DTIC FILE COPY

AD-A190 701

INTERIM PROGRESS REPORT

FOR THE PERIOD

16 OCTOBER 1987 THROUGH 15 DECEMBER 1987

FOR THE PROJECT

"COMPOSITE CERAMIC SUPERCONDUCTING  
FILAMENTS FOR SUPERCONDUCTING CABLE"

CONTRACTOR

CERAMICS PROCESS SYSTEMS CORPORATION  
840 MEMORIAL DRIVE  
CAMBRIDGE, MASSACHUSETTS 02139

DTIC  
SELECTED  
JAN 22 1988  
S D

DISTRIBUTION STATEMENT A  
Approved for public release  
Distribution Unlimited



**CERAMICS**  
PROCESS SYSTEMS

(4)

INTERIM PROGRESS REPORT

FOR THE PERIOD

16 OCTOBER 1987 THROUGH 15 DECEMBER 1987

FOR THE PROJECT

"COMPOSITE CERAMIC SUPERCONDUCTING  
FILAMENTS FOR SUPERCONDUCTING CABLE"

CONTRACTOR

CERAMICS PROCESS SYSTEMS CORPORATION  
840 MEMORIAL DRIVE  
CAMBRIDGE, MASSACHUSETTS 02139

5 JANUARY 1988

ARPA ORDER NO: 6214  
CONTRACT NO: N00014-87-C-0789  
CONTRACT EFFECTIVE DATE: 16 AUGUST 1987  
CONTRACT EXPIRATION DATE: 15 JANUARY 1988  
PRINCIPAL INVESTIGATOR: JOHN W. HALLORAN  
(617) 354-2020

DEFENSE  
ELECTRONICS  
S JAN 22 1988

Prepared for  
DEFENSE ADVANCED RESEARCH PROJECTS AGENCY  
1400 Wilson Boulevard  
Arlington, VA 22209

at D

OFFICE OF NAVAL RESEARCH  
800 North Quincy Street  
Arlington, VA 22217-5000

APPROVED FOR PUBLIC RELEASE: DISTRIBUTION IS UNLIMITED

The views and conclusions contained in this document are those of the authors and should not be interpreted as necessarily representing the official policies, either expressed or implied, of the Defense Advanced Research Projects Agency or the U. S. Government.

UNCLASSIFIED

SECURITY CLASSIFICATION OF THIS PAGE

REPORT DOCUMENTATION PAGE

1a. REPORT SECURITY CLASSIFICATION UNCLASSIFIED		1b. RESTRICTIVE MARKINGS N/A	
2a. SECURITY CLASSIFICATION AUTHORITY N/A		3. DISTRIBUTION/AVAILABILITY OF REPORT Approved for public release Distribution Unlimited	
2b. DECLASSIFICATION/DOWNGRADING SCHEDULE N/A		5. MONITORING ORGANIZATION REPORT NUMBER(S) N/A	
4. PERFORMING ORGANIZATION REPORT NUMBER(S) N/A		7a. NAME OF MONITORING ORGANIZATION Office of Naval Research	
6a. NAME OF PERFORMING ORGANIZATION Ceramics Process Systems Corporation	8a. OFFICE SYMBOL (If applicable) N/A	7b. ADDRESS (City, State and ZIP Code) 800 North Quincy Street Arlington, VA 22217-5000	
6b. ADDRESS (City, State and ZIP Code) 840 Memorial Drive Cambridge, MA 02139		9. PROCUREMENT INSTRUMENT IDENTIFICATION NUMBER Contract #N00014-87-C-0789	
8b. NAME OF FUNDING/SPONSORING ORGANIZATION Defense Advanced Research Projects Agency	8c. OFFICE SYMBOL (If applicable) N/A	10. SOURCE OF FUNDING NOS.	
8c. ADDRESS (City, State and ZIP Code) 1400 Wilson Boulevard Arlington, VA 22209		PROGRAM ELEMENT NO.	PROJECT NO.
11. TITLE (Include Security Classification) Ceramic Superconductor Filaments		TASK NO.	WORK UNIT NO.
12. PERSONAL AUTHOR(S) John W. Halloran			
13a. TYPE OF REPORT Progress Report	13b. TIME COVERED FROM 10/16/87 to 12/15/87	14. DATE OF REPORT - Yr., Mo., Day 87 January 5	15. PAGE COUNT 7
16. SUPPLEMENTARY NOTATION N/A			
17. COSATI CODES		18. SUBJECT TERMS (Continue on reverse if necessary and identify by block numbers)	
FIELD	GROUP	SUB. GR.	Superconductor, Ceramic, <i>Ceramic</i>
			<i>William, B...</i>
19. ABSTRACT (Continue on reverse if necessary and identify by block numbers)  SEE ATTACHED			
20. DISTRIBUTION/AVAILABILITY OF ABSTRACT UNCLASSIFIED/UNLIMITED <input checked="" type="checkbox"/> SAME AS RPT <input type="checkbox"/> OTIC USERS <input type="checkbox"/>		21. ABSTRACT SECURITY CLASSIFICATION Unclassified	
22a. NAME OF RESPONSIBLE INDIVIDUAL John W. Halloran		22b. TELEPHONE NUMBER (Include Area Code) 617-354-2020	22c. OFFICE SYMBOL N/A

UNCLASSIFIED

SECURITY CLASSIFICATION OF THIS PAGE

## ABSTRACT

This is the second progress report of a five month program to demonstrate the feasibility of manufacturing superconducting wires from  $\text{YBa}_2\text{Cu}_3\text{O}_{7-x}$ , consisting of a small ceramic core with a copper cladding. The ceramic core is to be produced from a dry spun ceramic fiber, sintered to create a  $\langle 010 \rangle$  fiber texture to enhance critical current. The sintered fiber is to be clad with copper by electroplating.

The sintering and microstructure development of  $\text{YBa}_2\text{Cu}_3\text{O}_{7-x}$  has been characterized for as-calcined and milled powder, both as undoped and doped with 5wt%  $\text{CuO}$ . The undoped powder reaches 94% density, with fully recrystallized grains after 15 hours at  $995^\circ\text{C}$ . The  $\text{CuO}$ -doped material sinters to full density at temperatures as low as  $925^\circ\text{C}$ , with extensive recrystallization. The resistivity has been measured as a function of temperature for nearly dense and relatively porous undoped material.

Fibers, produced by dry spinning  $\text{YBa}_2\text{Cu}_3\text{O}_{7-x}$ , can be nearly fully densified by a rapid zone sintering process. Total dwell time at peak temperature of 4-10 minutes is sufficient to densify both undoped and  $\text{CuO}$ -doped fibers. Continuous fiber sintering appears to be practical using a scaled-up version of the zone sintering process. After an oxygen intercalation anneal, the sintered fibers are superconducting.

The zone sintering is used to attempt to develop microstructural texture by directional recrystallization. Early results indicate the  $\langle 010 \rangle$  particle axes seem to align at 45 degrees to the fiber axis, rather than colinear with the fiber axis. This method, and other texturing methods are being further developed.

Usable fibers are being dry spun in about one meter lengths. With the current apparatus, the fibers are in fact spun continuously, but can only be collected in short lengths due to inadequate drying. The collected fiber, however, is adequate in quality and quantity for present experimental purposes. The spinnability of the dry spinning dope has been related to the viscoelastic behavior, as determined by dynamic mechanical analysis.

COMPOSITE CERAMIC SUPERCONDUCTING  
FILAMENTS OF SUPERCONDUCTING CABLE

ABSTRACT

This is the second progress report of a five month program to demonstrate the feasibility of manufacturing superconducting wires from  $\text{YBa}_2\text{Cu}_3\text{O}_{7-x}$ , consisting of a small ceramic core with a copper cladding. The ceramic core is to be produced from a dry spun ceramic fiber, sintered to create a  $\langle 010 \rangle$  fiber texture to enhance critical current. The sintered fiber is to be clad with copper by electroplating.

The sintering and microstructure development of  $\text{YBa}_2\text{Cu}_3\text{O}_{7-x}$  has been characterized for as-calcined and milled powder, both as undoped and doped with 5wt% CuO. The undoped powder reaches 94% density, with fully recrystallized grains after 15 hours at 995°C. The CuO-doped material sinters to full density at temperatures as low as 925°C, with extensive recrystallization. The resistivity has been measured as a function of temperature for nearly dense and relatively porous undoped material.

Fibers, produced by dry spinning  $\text{YBa}_2\text{Cu}_3\text{O}_{7-x}$ , can be nearly fully densified by a rapid zone sintering process. Total dwell time at peak temperature of 4-10 minutes is sufficient to densify both undoped and CuO-doped fibers. Continuous fiber sintering appears to be practical using a scaled-up version of the zone sintering process. After an oxygen intercalation anneal, the sintered fibers are superconducting.

The zone sintering is used to attempt to develop microstructural texture by directional recrystallization. Early results indicate the  $\langle 010 \rangle$  particle axes seem to align at 45 degrees to the fiber axis, rather than colinear with the fiber axis. This method, and other texturing methods are being further developed.

Usable fibers are being dry spun in about one meter lengths. With the current apparatus, the fibers are in fact spun continuously, but can only be collected in short lengths due to inadequate drying. The collected fiber, however, is adequate in quality and quantity for present experimental purposes. The spinnability of the dry spinning dope has been related to the viscoelastic behavior, as determined by dynamic mechanical analysis.



Accession For	
NTIS (CRA&I)	<input checked="" type="checkbox"/>
DTIC TAB	<input type="checkbox"/>
Unannounced	<input type="checkbox"/>
Justification	
By	
Date	
Availability	
Distribution	
Notes	
A-1	

## TABLE OF CONTENTS

ABSTRACT.....	iv
LIST OF FIGURES.....	vi
LIST OF TABLES.....	x
1. INTRODUCTION.....	1
2. $\text{YBa}_2\text{Cu}_3\text{O}_{7-x}$ POWDER PREPARATION AND SINTERING.....	3
2.1 $\text{YBa}_2\text{Cu}_3\text{O}_{7-x}$ Powder Production.....	3
2.2 Powder Characteristics and Sintering.....	6
2.2.1 Introduction.....	6
2.2.2 Sintering of $\text{YBa}_2\text{Cu}_3\text{O}_{7-x}$ Pellets.....	7
2.2.3 Zone Sintering of $\text{YBa}_2\text{Cu}_3\text{O}_{7-x}$ Fibers.....	22
2.2.4 Compatability Test.....	36
3. MICROSTRUCTURAL TEXTURE.....	38
3.1 Green Texture.....	38
3.2 Directional Recrystallization Experiments.....	39
4. ELECTRICAL MEASUREMENTS.....	49
5. FIBER SPINNING DEVELOPMENT.....	53
5.1 Fiber Spinning Developments.....	53
5.2 $\text{YBa}_2\text{Cu}_3\text{O}_{7-x}$ Fiber Spinning.....	55
5.3 Continuous Spinning Developments.....	63
5.4 Viscoelastic Investigation of Spinning Dope.....	66
5.4.1 Dynamic Mechanical Analysis.....	69
5.4.2 Measurements on Spinning Dope.....	70
6. METAL CLADDING.....	77
7. SUMMARY AND CONCLUSIONS.....	78



## LIST OF FIGURES

Figure 2.1A	YBa <sub>2</sub> Cu <sub>3</sub> O <sub>7-x</sub> Particles in Freeze-Dried Granule Calcined 16.5 hours at 900°C Batch 24729	10,000X.....8
Figure 2.1B	YBa <sub>2</sub> Cu <sub>3</sub> O <sub>7-x</sub> Particles after Vibromilling 24.5 hours in Cyclohexane	15,000X.....8
Figure 2.2	Density vs. Sintering Temperature for Pellets Sintered 15 hours.....	10
Figure 2.3A	Fracture Surface of Pellet of As-Calcined Powder A Sintered 15 hours at 975°C	1000X.....12
Figure 2.3B	Fracture Surface of Pellet of Powder B, Doped with 5 wt% CuO, Sintered 15 hours at 975°C	1000X.....13
Figure 2.3C	Fracture Surface of Pellet of Milled Powder C Sintered 15 hours at 975°C	1000X.....14
Figure 2.4	Fracture Surface of CuO-Doped Powder B Sintered 15 hours at 975°C	100X.....15
Figure 2.5	Optical Micrograph of Pellet of CuO-Doped Powder B Sintered 15 hours at 985°C crossed polars, 400X.....	18
Figure 2.6	Optical Micrograph of Pellet of Milled Powder C Sintered 15 hours at 995°C	1000X.....19
Figure 2.7	Density vs. Temperature for As-Calcined and Milled YBa <sub>2</sub> Cu <sub>3</sub> O <sub>7-x</sub> Sintered 15 hours.....	20
Figure 2.8	Fiber of CuO-Doped Composition Sintered 15 hours at 965°C in Oxygen	800X.....21
Figure 2.9	Temperature - Time Record for a Zone Sintering Experiment.....	23

Figure 2.10	YBa <sub>2</sub> Cu <sub>3</sub> O <sub>7-x</sub> Particles in Green Fiber after Binder Burnout Above: Fiber 24434, with Dry Vibromilled Powder Below: Fiber 26809, with Cyclohexane Milled Powder 10,000X.....	24
Figure 2.11	Surface of Undoped Fiber 24434 Zone Sintered at 998°C Right: one pass Left: two passes 5000X.....	29
Figure 2.12	Fracture Surface of Undoped Fiber 24434 After Two Passes at 998°C 5000X.....	29
Figure 2.13	Undoped Fiber 24434 Zone Sintered for Three Passes At 998°C Above: Cross-section Below: Surface 2000X.....	30
Figure 2.14	Fracture Surface of CuO-Doped Specimen 24950B Zone Sintered for Two Passes at 989°C 1000X.....	31
Figure 2.15	Surface of CuO-Doped Fiber after Ten Zone Sintering Passes at 989°C Specimen 24950C 2000X.....	32
Figure 2.16A	CuO-Doped Fiber Presintered 37 Minutes at 925°C 2000X.....	33
Figure 2.16B	CuO-Doped Fiber Presintered 37 Minutes at 925°C and Zone Sintered for Six Passes at 971°C 2000X.....	33
Figure 2.17A	Cross-Section of CuO-Doped Fiber Presintered Two Hours at 950°C and Zone Sintered for Six Passes at 971°C 2000X.....	34
Figure 2.17B	Surface of CuO-Doped Fiber Presintered Two Hours at 950°C and Zone Sintered for Six Passes at 971°C 2000X.....	35
Figure 3.1	Polished Section of Undoped Fiber 24434 Zone Sintered for Three Passes at 998°C crossed polars 400X.....	44
Figure 3.2	Polished Section of CuO-Doped Fiber Zone Sintered Ten Passes at 989°C and Oxygen Annealed at 500°C crossed polars 400X.....	45

Figure 3.3	Twinning in CuO-Doped Fiber Zone Sintered Ten Passes at 989°C and Oxygen Annealed at 500°C crossed polars 1000X.....	46
Figure 3.4	Distributions of Measured Angles between Fiber Axis and Traces of Grain Habit Planes for a CuO- Doped 26809 Fiber (Specimen 50C) and Undoped 24434 Fiber (Specimen 22A).....	47
Figure 3.5	Polished Section of CuO-Doped Fiber Sintered Isothermally for 15 hours at 965°C crossed polars 400X.....	48
Figure 4.1	Fracture Surface of the 94% Dense Undoped Specimen Used for Resistivity Measurements 300X.....	51
Figure 4.2	Resistivity vs. Temperature for Undoped Pellets at 75% and 94% Theoretical Density.....	52
Figure 5.1	Top: Barium Titanate Green Fibers Bottom: $\text{YBa}_2\text{Cu}_3\text{O}_{7-x}$ Green Fibers 6.5X.....	54
Figure 5.2	$\text{YBa}_2\text{Cu}_3\text{O}_{7-x}$ Fiber from Formulation 24484-1, Using Dry Vibromilled Powder, With Non-uniform Diameter 100X.....	60
Figure 5.3	$\text{YBa}_2\text{Cu}_3\text{O}_{7-x}$ Green Fiber from Formulation 26801, Using Cyclohexane Vibromilled Powder Top: 600X Bottom: 100X.....	61
Figure 5.4	$\text{YBa}_2\text{Cu}_3\text{O}_{7-x}$ Green Fiber from Formulation 26817 Top: 600X Bottom: 100X.....	62
Figure 5.5	Barium Titanate Green Fibers at Varying Spinning Conditions. See Text.....	68
Figure 5.6A	Dynamic Mechanical Analysis Experiment.....	72
Figure 5.6B	Viscoelastic Response of a Typical Polymer Melt Showing Flow Region at Low Frequencies, where Loss Modulus $G''$ exceeds Storage Modulus $G'$ , Rubbery Plateau at Intermediate Frequencies, and Glass Region at High Frequencies.....	72
Figure 5.7	Viscoelastic Response of Standard Spinning Dope Formulation 24424-1 Milled 18 hours.....	73



LIST OF TABLES

Table 2.1	Wet Chemical Analysis of Powder Dry Vibromilled YBa <sub>2</sub> Cu <sub>3</sub> O <sub>7-x</sub> Powder 21496B After Classification....5
Table 5.1	Standard Green Fiber Spinning Dope Formulation...58
Table 5.2	YBa <sub>2</sub> Cu <sub>3</sub> O <sub>7-x</sub> Fiber Formulations.....59
Table 5.3	Fiber Diameter At Different Spinning Conditions..67

## INTERIM PROGRESS REPORT

COMPOSITE CERAMIC SUPERCONDUCTING FILAMENTS FOR SUPERCONDUCTING CABLE

J.W. HALLORAN, L.J. KLEMPNER, R.J. PICERNO,

Z. CHEN, AND K. VENKATASWAMY

CERAMICS PROCESS SYSTEMS CORPORATION, CAMBRIDGE, MASSACHUSETTS

## SECTION 1

## INTRODUCTION

This is the second Interim Progress Report on a program at the Ceramics Process Systems Corporation to develop practical manufacturing methods for composite superconducting wires using the ceramic superconductor  $\text{YBa}_2\text{Cu}_3\text{O}_{7-x}$ . This research is supported with a five month contract from the Office of Naval Research (Contract Number N00014-87-C-0789) starting 16 August 1987 and expiring 15 January 1988.

This development program is aimed at the fabrication of composite superconducting filaments consisting of a core of high  $J_c$  ceramic superconductor, and a cladding of strong, high conductivity copper metal. The approach is to fabricate  $\text{YBa}_2\text{Cu}_3\text{O}_{7-x}$  ceramic fiber by dry spinning, sinter the fiber to an optimum microstructure for superconducting

properties, adjust the oxygen content, and subsequently clad the fiber with copper or other metals with an ambient temperature process.

Specifically, the objectives of this program are to:

1. Define and demonstrate fiber drawing and sintering processes with potential for continuous fiber manufacture,
2. Demonstrate the production of a textured microstructure
3. Correlate microstructure with critical current measurements, and
4. Demonstrate proof-of-principle for copper cladding.

This Interim Progress Report covers the period 16 October through 15 December 1987. Research effort in this period focused on fabricating longer lengths of ceramic fiber and developing a rapid sintering process compatible with a practical continuous sintering process. Powder production techniques were further refined, and scaled-up. The sintering behavior of the powder was characterized in more detail. Work was begun in earnest on characterizing texture in fiber specimens sintered in "directional recrystallization" experiments. Resistivity vs. temperature measurements are reported for an early apparatus, and the equipment has been upgraded. No significant work on metal cladding was performed in this period. The principal research team for this report period included L. J. Klemptner, R. J. Picerno, K. Venkataswamy, Z. Chen, and J. Halloran.

## SECTION 2

YBa<sub>2</sub>Cu<sub>3</sub>O<sub>7-x</sub> POWDER PREPARATION AND SINTERING2.1 YBa<sub>2</sub>Cu<sub>3</sub>O<sub>7-x</sub> POWDER PRODUCTION

Efforts in powder production during this period involved routine production of a standard powder, and attempts to improve and scale-up the calcination process. Only minor changes were made in the process described in the previous report. This involved preparing the raw oxide mixture by vibromilling in water with zirconia media to produce a specific surface area of 5-6 m<sup>2</sup>/gm. The apparent median "particle size" obtained by sedimentation analysis of this mixture is 1.9 +/-0.5 microns after 22 hours of vibromilling. The milled mixture is granulated by spraying droplets of the stirred suspension in liquid nitrogen to produce frozen granules. The granules are desiccated by freeze drying. The granulated powder is loaded into an alumina crucible in 250 gm batches and calcined 15 hours at 900°C. Oxygen or air is introduced into the bottom of the crucible with a lance so that there is a steady flow of gas throughout the bed of granules.

This process was reasonably reproducible, although two seemingly minor changes caused poor results. The original freeze-dried granules were rather fragile, and a fraction of the granulated batch was lost upon handling. To remedy this situation, 1.00-1.24 wt% of binder<sup>1</sup> was added to the aqueous slurry before freeze granulation. Unfortunately, the batch

---

<sup>1</sup>. Polyethylene Glycol, 600 molecular weight. Carbowax 600, Union Carbide Corporation, Danbury, CT



with binder required different calcination conditions, and a number of trials were needed before phase pure  $\text{YBa}_2\text{Cu}_3\text{O}_{7-x}$  could be produced. Another change was the solids content in the suspension used for granulation, which was increased in a process "improvement". The denser granules calcined well, but were much more difficult to crush. After a number of trials, the original lower solids content was re-established to restore the desirable friability of the calcined granules.

As an intermediate scale-up, we have attempted to run four 250 gram crucibles simultaneously, using a four-pronged manifold to supply oxygen to four crucibles from a single line. Unfortunately, at least one of the four crucibles contained grey incompletely reacted materials. Numerous experiments were tried to adjust the manifold to get uniform flow, always with encouraging but imperfect results. Most recently we have been trying a single larger crucible, which can do a 600 gram batch. After a number of experiments, in which the air flow rate was either too fast or too slow, this larger crucible process seems to be almost perfected.

Our powder production is satisfactory, but represents a drain of resources which could be deployed elsewhere if a good commercial powder were available. Two commercial powders have been ordered, but have not yet arrived.

Several samples of  $\text{YBa}_2\text{Cu}_3\text{O}_{7-x}$  have been sent out for wet chemical analysis, but at present only one set of data is available. These data are for powder 21496B, an early calcine lot which had been dry vibromilled with zirconia media for 24.5 hours. This powder was later dispersed in toluene using sorbitan trioleate as a dispersant, and classified by gravitational sedimentation into a coarse cut with stokes diameter greater than 5

microns, an fine cut with stokes diameters between 3 and 5 microns, and a superfine cut finer than 3 microns. The chemical composition of the coarse and superfine cuts are shown in Table 2.1. The reproducibility of the analysis can be assessed by comparing the two trials for the coarse powder. The average of these two has the copper/yttrium mole ratio at  $3.02 \pm 0.07$  and the barium/yttrium mole ratio at  $2.09 \pm 0.07$ , within experimental error of the 1-2-3 composition. The corresponding mole ratios for the fine fraction of this powder are somewhat lower, suggesting slight yttrium enrichment, although the difference may be within experimental error.

Table 2.1

## Wet Chemical Analysis of Coarse and Superfine Classified 21496B

<u>Cut</u>	<u>Trial #</u>	<u>Element</u>	<u>Wt%</u>	<u>mole ratio</u>
Coarse >5 microns	1	Cu	25.9	2.95
		Ba	38.3	2.02
		Y	12.3	1
Coarse >5 microns	2	Cu	25.7	3.09
		Ba	38.5	2.15
		Y	11.6	1
Superfine ≤3 microns	1	Cu	26.3	2.81
		Ba	39.7	1.96
		Y	13.1	1

## 2.2 POWDER CHARACTERISTICS AND SINTERING

### 2.2.1 Introduction

During this report period we have studied the sintering of pellets of  $\text{YBa}_2\text{Cu}_3\text{O}_{7-x}$  powder in some detail, and conducted a number of sintering experiments on early  $\text{YBa}_2\text{Cu}_3\text{O}_{7-x}$  fibers. The pellet experiments were primarily to examine density and grain size as a function of temperature, time, and atmosphere. These are conventional furnace experiments involving slow heating, extended sintering anneals up to 15 hours long, and slow cooling to the oxygen intercalation anneal temperature. This work is comparable to reports in the literature. We have used pellets to look at the effects of particle size, and compare undoped  $\text{YBa}_2\text{Cu}_3\text{O}_{7-x}$  with  $\text{YBa}_2\text{Cu}_3\text{O}_{7-x}$  doped with 5 wt%  $\text{CuO}$ . It is much easier to handle pellets and measure their density, compared to the tiny fibers. Pellet sintering acts as a tool to test powder quality, and provides specimens to cut bars for electrical measurements.

Fiber sintering experiments were undertaken as fiber became available. Most of these experiments are quite different in their goals. Here we attempt to sinter the fibers in a way which simulates a continuous sintering process. The objective is to use a small laboratory furnace and short pieces of fiber to determine the temperature-time profile required to sinter continuous lengths of fiber. This profile must be known to properly design the continuous sintering facility. The initial activity involves developing a profile consistent with the fiber sintering behavior. As we develop procedures to characterize the electrical properties of these

fibers, we will refine the profile to optimize the superconducting properties.

We find that the fibers can be successfully densified very rapidly, with total dwell time at temperature of only a few minutes. This indicates that continuous sintering is practical, and can yield a reasonable throughput from conventionally-sized sintering furnaces. Removal of the binder in the green fiber does not seem to be a difficult problem. It appears likely that the fibers must be supported during sintering. This raises the potential of undesirable reaction between the  $\text{YBa}_2\text{Cu}_3\text{O}_{7-x}$  and the support material. However, the rapid sintering works in our favor here. Preliminary indications suggest that the  $\text{YBa}_2\text{Cu}_3\text{O}_{7-x}$  fibers can be sintered on alumina ceramic and felt, zirconia ceramic, chromel alloy, and Nextel 312 refractory fabric without noticeable reaction after the several minutes necessary for densification. This is in sharp contrast to the situation with long sintering anneals typical of our pellet sintering, in which vigorous reaction occurs with these materials.

#### 2.2.2. Sintering of $\text{YBa}_2\text{Cu}_3\text{O}_{7-x}$ Pellets

The bulk of the sintering experiments on pellets performed during this period involved a comparison of the sintering behavior of three powders: powder A, the standard as-calcined powder from batch number 24729; powder B, which is powder from the same batch 24729 mixed with an extra 5 wt%  $\text{CuO}$  after calcination; and powder C, a standard powder from batch number 24707, which had been wet milled in cyclohexane. Powders A and B were relatively coarse, having a specific surface area of only  $0.7 \text{ m}^2/\text{gm}$  characteristic of the calcined material. Figure 2.1A shows the 1-3 micron platey  $\text{YBa}_2\text{Cu}_3\text{O}_{7-x}$



Figure 2.1A YBa<sub>2</sub>Cu<sub>3</sub>O<sub>7-x</sub> Particles in Freeze-Dried Granule  
Calcined 16.5 hours at 900°C Batch 24729 10,000X

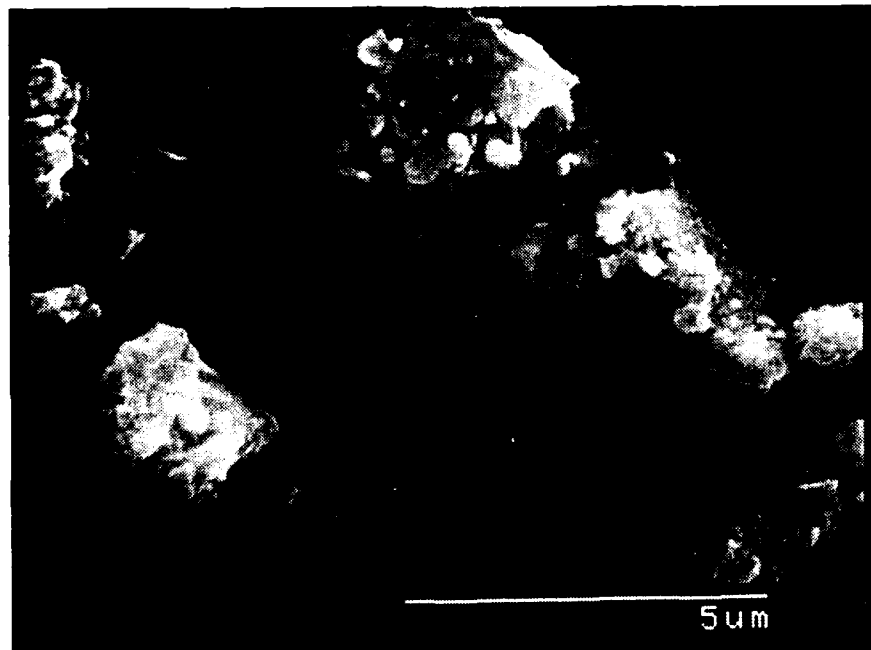


Figure 2.1B YBa<sub>2</sub>Cu<sub>3</sub>O<sub>7-x</sub> Particles after Vibromilling 24.5 hours  
in Cyclohexane 15,000X

particles in the freeze dried granule after calcination. These powders were not milled after calcination, but were lightly ground by hand in a mortar and pestle to crush the granules. The powder consists of hard agglomerates much larger than the primary particles shown in Figure 2.1A. The copper oxide addition to powder B was made during this hand grinding. Powder C was vibromilled in cyclohexane for 24.5 hours using zirconia milling media. Figure 2.1B shows the rather angular particles created by the milling treatment. Vibromilling increased the specific surface area to  $2.2 \text{ m}^2/\text{gm}$  and reduced the median particle size to 2.0 microns, as determined by centrifugal sedimentation using a Horiba particle sizing instrument. Powders A and B were too coarse to analyze with the Horiba.

Pellets were prepared by dry pressing one gram charges of these powders at 20,000 psi in a 0.5 inch diameter steel die. The pellets were supported on a loose bed of  $\text{YBa}_2\text{Cu}_3\text{O}_{7-x}$  powder, and sintered in a box furnace into which oxygen was bled at a rate of 77 ml STP/minute. Eight sintering temperatures between 925 and 995°C were examined, with the following schedule: heat 5°C/minute to maximum temperature, hold 15 hours, cool at 5°C/minute to 500°C, hold 2 hours, cool 25°C/minute to room temperature. The densities of the sintered pellets were measured using a standard immersion method with isopropanol, and expressed as percent theoretical density using a value of  $6.2 \text{ gm/cm}^3$  as the theoretical density of all specimens. All of the sintered pellets exhibited a Meissner effect as indicated by levitation over a magnet.

The sintering data is displayed in Figure 2.2. The as-calcined powder A undergoes very little sintering at 925°C, but improves rapidly as

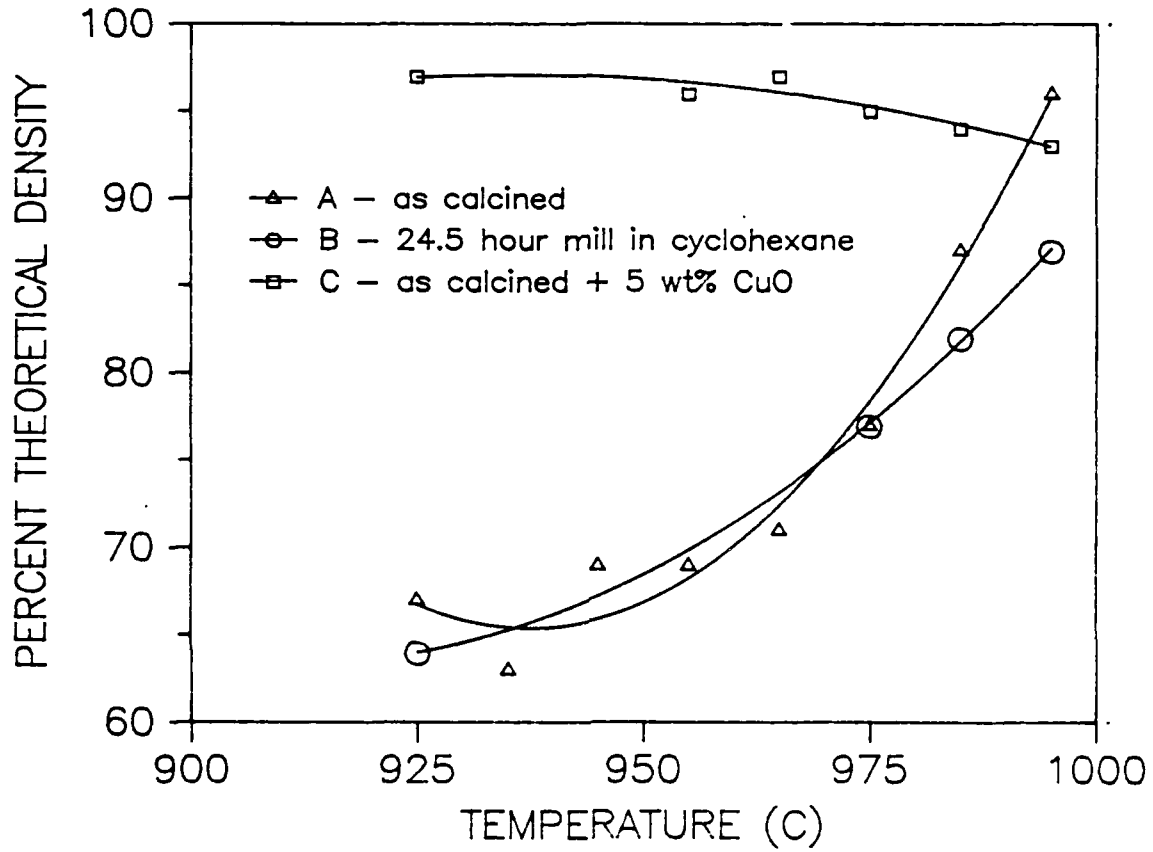


Figure 2.2 Density vs. Sintering Temperature for Pellets Sintered 15 hours

temperature increases, achieving 96% density at 995°C. Similar results are obtained for several other batches of as-calcined powder. Milling in cyclohexane did not improve the sinterability, which is surprising in view of the three-fold increase in specific surface area of the milled powder C. Except for one point at 965°C, the milled powder C achieved lower densities than powder A. The highest density obtained from powder C was only 85% theoretical at 995°C. The effect of excess copper oxide as a sintering aid is shown by the consistently high densities achieved by powder B, the as-calcined powder with 5 wt% added CuO. This powder reached 97% density at 925°C. The density decreases somewhat at higher temperatures, probably due to pore entrapment associated with the very extensive secondary recrystallization that occurred at higher temperatures, where tabular grains hundreds of microns long were commonplace.

The microstructures of the pellets sintered at 975°C are compared in Figure 2.3 A, B, and C, which show fracture surfaces at 1000x magnification. Powder A and the milled powder B are very similar at this temperature. Both are about 78% dense with 2-3 micron grains, which is close to the starting particle size of powder B. The difference in the microstructure of the copper-rich powder is striking, as shown in Figure 2.3C. The extensive recrystallization is better seen at lower magnification. Figure 2.4 shows the same specimen at 100x, in which massive grains up to 500 microns long are visible. High density is associated with extensive grain growth in the as-calcined powder A as well. Fracture surfaces of the 94% dense pellet sintered at 995°C show tabular grains more than 100 microns long (see Figure 4.1, Section 4).



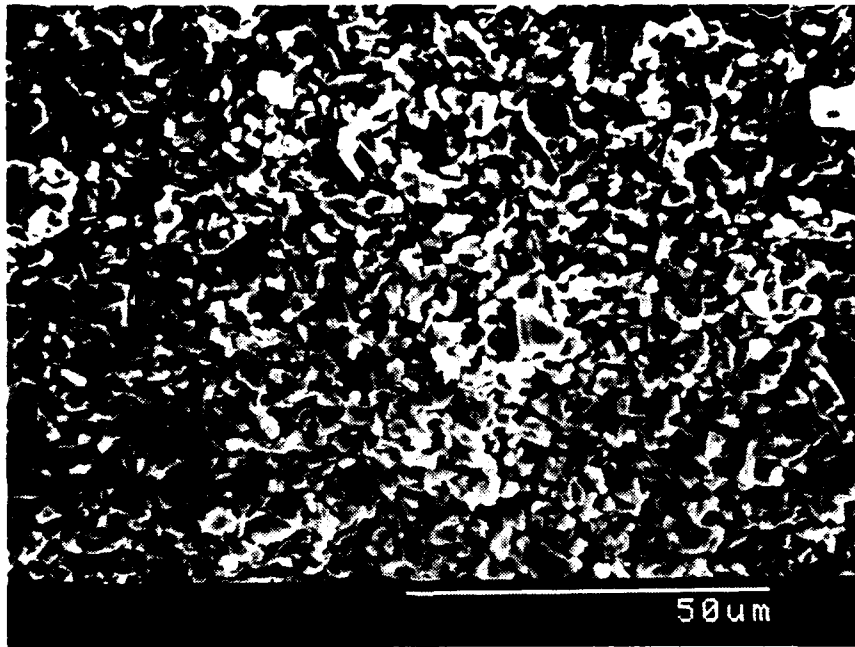


Figure 2.3A Fracture Surface of Pellet of As-Calcined  
Powder A Sintered 15 hours at 975°C  
1000X

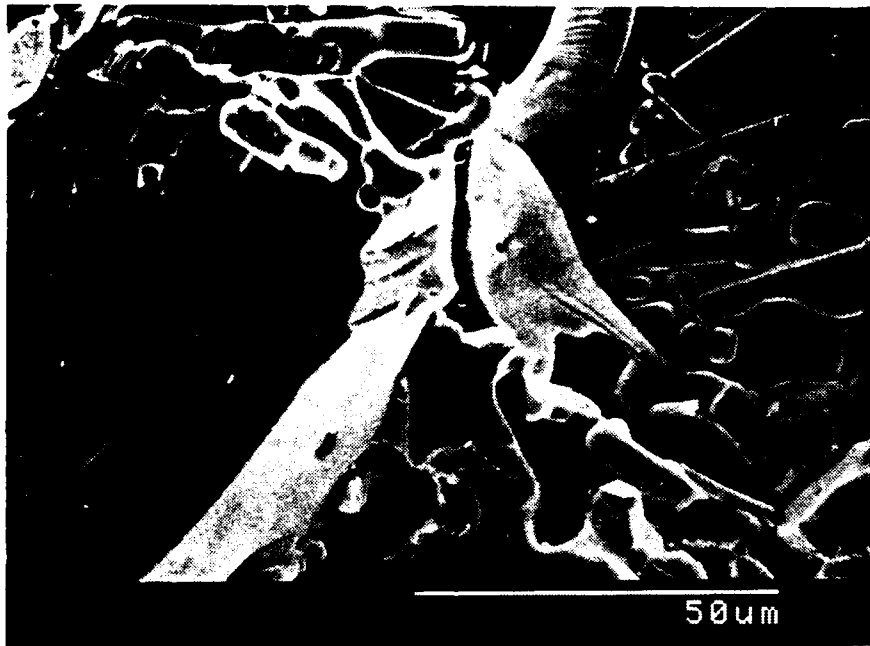


Figure 2.3B Fracture Surface of Pellet of Powder B, Doped  
with 5 wt% CuO, Sintered 15 hours at 975°C  
1000X

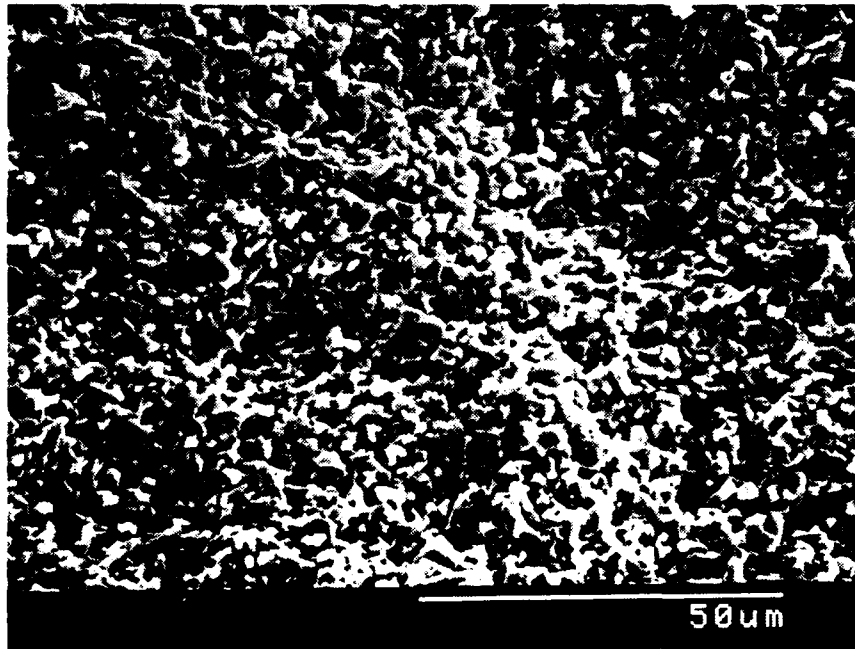


Figure 2.3C      Fracture Surface of Pellet of Milled Powder C  
Sintered 15 hours at 975°C  
1000X



Figure 2.4 Fracture Surface of CuO-Doped Powder B  
Sintered 15 hours at 975°C  
100X

Optical micrographs of the large grained copper rich material shows the platey habit of the  $\text{YBa}_2\text{Cu}_3\text{O}_{7-x}$  planes more clearly. Under crossed polars the twin structure of the orthorhombic phase is visible. Figure 2.5 show the powder B specimen sintered at  $985^\circ\text{C}$  for 15 hours. The spacing of these optical twins is variable, and most of the larger grains have several domains. Twinning is not visible in the polished section of the porous powder C pellet. The 85% dense pellet sintered at  $995^\circ\text{C}$  is shown in Figure 2.6. This specimen did not polish well, and the fine grains are difficult to resolve optically.

The insensitivity of the sintering of the undoped powder to gentle milling treatments is further illustrated in Figure 2.7. This shows the density achieved by 15 hour sintering anneals as a function of temperature. The sintering behavior of the as-calcined powder (batch 24729) is compared with powder from a similar batch (24718) which had been vibromilled in cyclohexane for 4.5 hours. Both powders have similar surface area, around  $0.6\text{m}^2/\text{gm}$  for the cyclohexane milled powder. The particle size distribution of the milled powder was determined by Sedigraph to be 90% finer than 6 microns, median 3 microns, and 10% finer than 1.2 microns. The as-calcined powder, after crushing in a mortar and pestle consisted largely of agglomerates larger than 10 microns. As shown in Figure 2.7, the sintering behavior of these powders is nearly identical.

More intensive milling can of course improve sinterability. In the previous report we described the sintering behavior of powder dry vibromilled to a surface area of  $12.5\text{m}^2/\text{gm}$ . These powders were highly

sinterable and produced a fine grain size ceramic. For example, sintering 15 hours at 925°C produced a 94% dense ceramic with 1-2 micron grain size, and, after oxygen annealing, an orthorhombic diffraction pattern. However this pellet was not superconducting. Samples from the calcined powder or the same batch before milling sinter like typical as-calcined powders, and are superconducting. It is not clear whether the absence of superconduction in the dry milled pellets is due to their fine grain size or if it is somehow related to the intensive dry vibromilling treatment. We have temporarily abandoned dry vibromilling.

#### Furnace Sintering of Fibers

To correlate the pellet sintering with fiber sintering, a sample of the first  $\text{YBa}_2\text{Cu}_3\text{O}_{7-x}$  fiber doped with 5 wt%  $\text{CuO}^2$  was sintered with the standard profile, for 15 hours at 965°C. Figure 2.8 shows the surface of two of these 60 micron diameter fibers. The grain growth is less extensive than in pellets sintered under similar conditions, probably because the fine fiber diameter suppresses the propagation of the very large grains. These fibers displayed a Meissner effect by the levitation test. For these long sintering profiles it was necessary to support the fibers on a bed of  $\text{YBa}_2\text{Cu}_3\text{O}_{7-x}$  granules. Fibers placed on alumina substrates reacted extensively, and much of the  $\text{CuO}$  was transported into the alumina, leaving the fiber as a porous relict of some unidentified phase.

---

<sup>2</sup>. Batch 26809, prepared with powder lot 24718, vibromilled in cyclohexane for 4.5 hours. See Section 3.

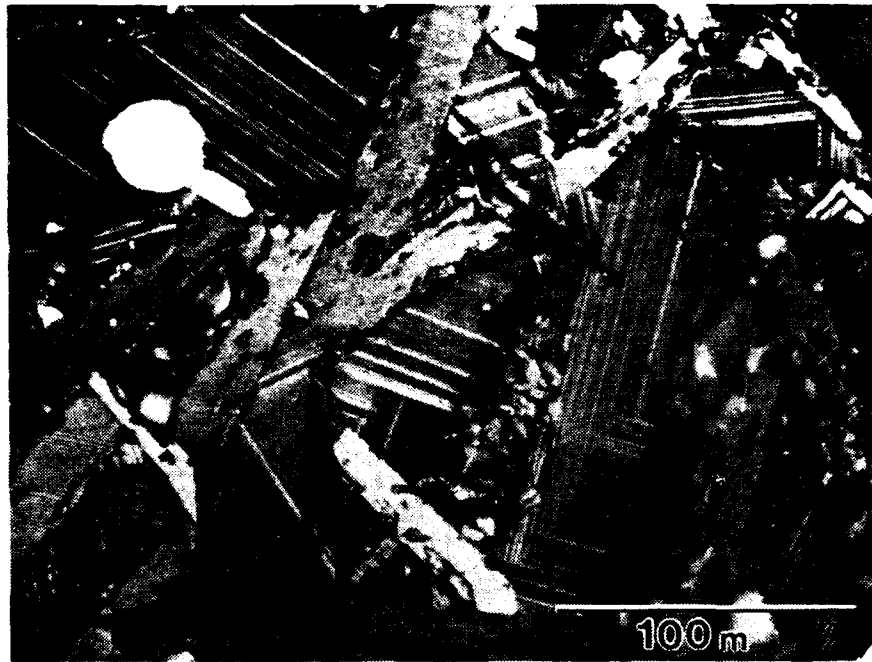


Figure 2.5      Optical Micrograph of Pellet of CuO-Doped  
Powder B Sintered 15 hours at 985°C  
crossed polars, 400X

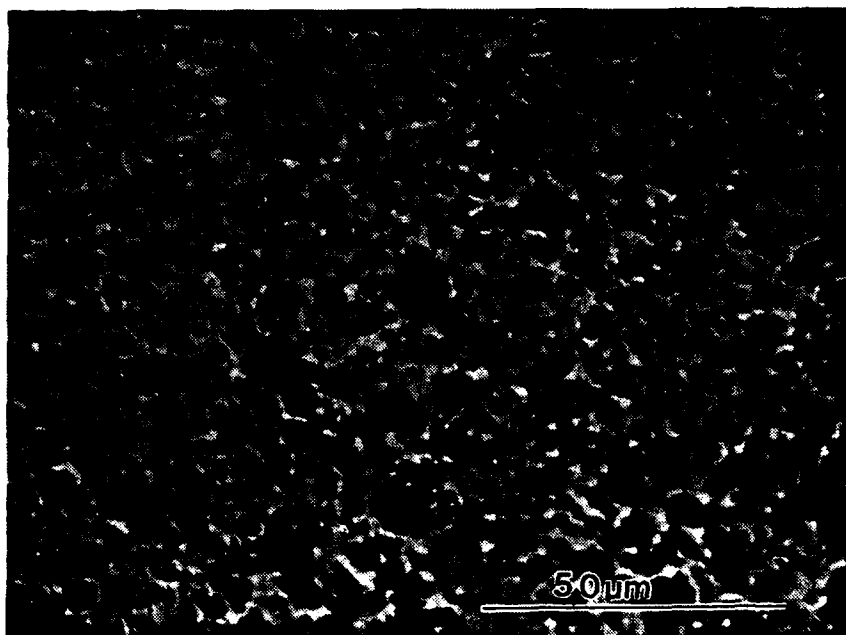


Figure 2.6      Optical Micrograph of Pellet of Milled Powder C  
Sintered 15 hours at 995°C  
1000X



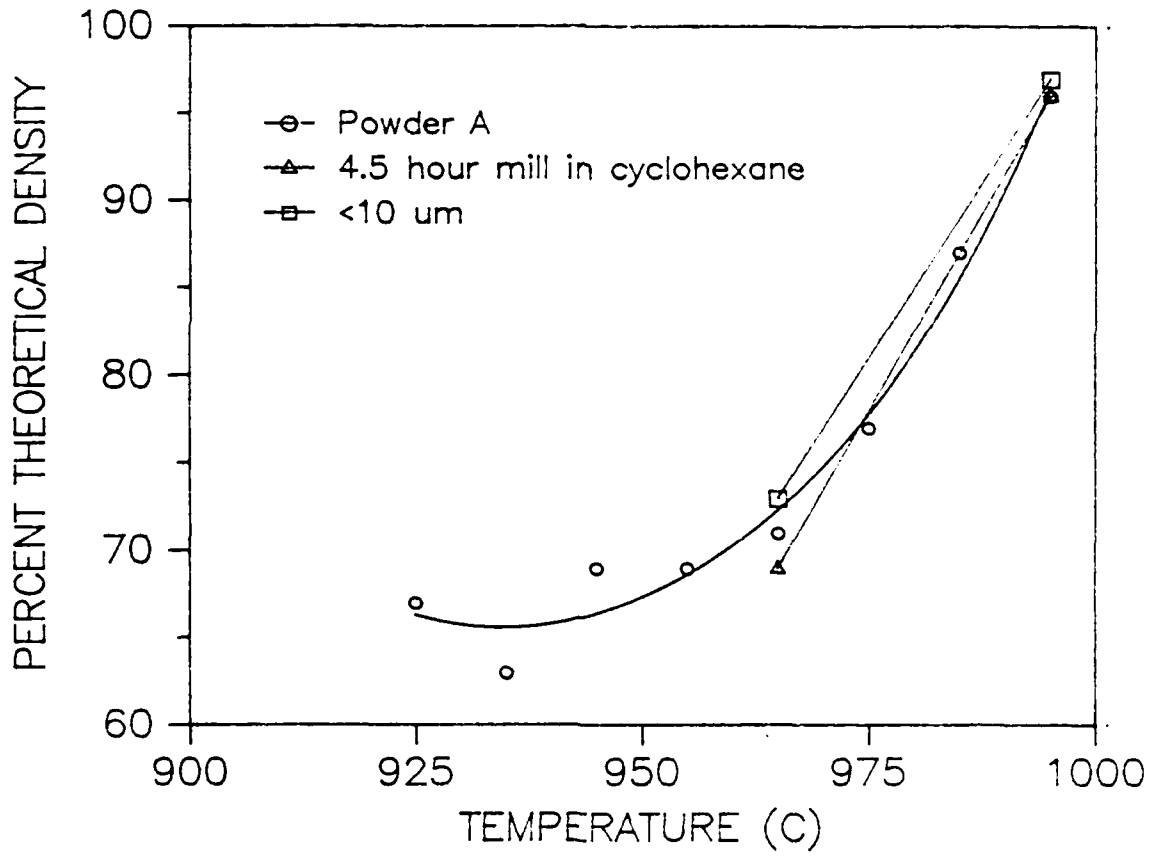


Figure 2.7 Density vs. Temperature for As-Calcined and Milled  $\text{YBa}_2\text{Cu}_3\text{O}_{7-x}$  Sintered 15 hours

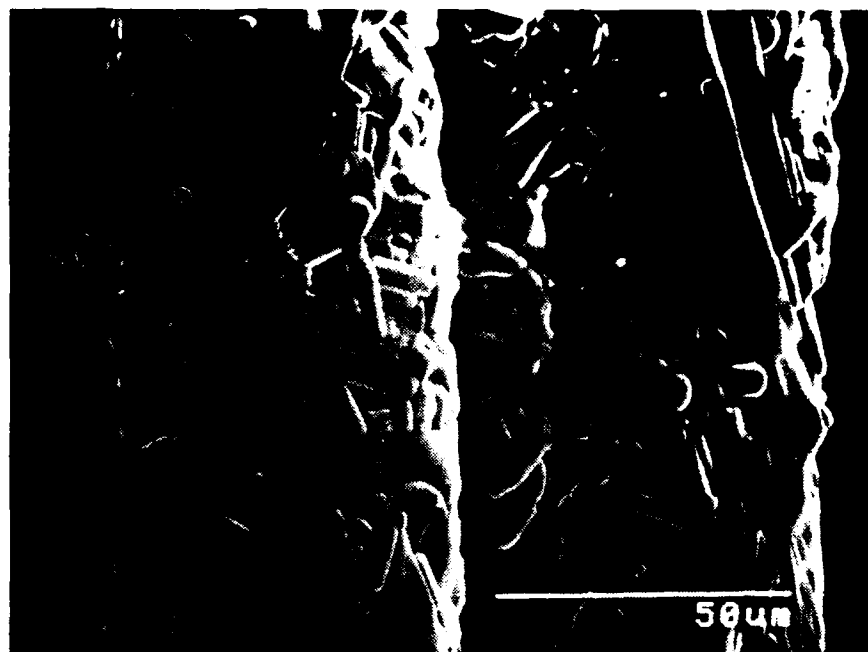


Figure 2.8 Fiber of CuO-Doped Composition Sintered 15 hours  
at 965°C in Oxygen 800X

### 2.2.3 Zone Sintering of $\text{YBa}_2\text{Cu}_3\text{O}_{7-x}$ Fibers

The zone sintering apparatus is a single zone horizontal tube furnace through which fiber specimens, supported on a very low thermal mass fixture, can be pushed at a controlled rate. The fiber specimens are supported on a setter which is typically 2 cm by 3 cm by 0.4 mm thick 99% alumina substrate<sup>3</sup>. Usually no reaction occurs between the fiber and the substrate during the brief sintering experiment. The specimen is moved through the furnace on a low thermal mass sled made from rigidized alumina fiber insulation<sup>4</sup>, which is attached to a long alumina push rod. The push rod is moved by a motorized device which can control the push rate between about 4 cm/minute and 150 cm/minute. Near the sintering range of  $\text{YBa}_2\text{Cu}_3\text{O}_{7-x}$ , the furnace has a uniform hot zone about 4 cm wide, with nearly linear temperature gradients of 7°C/cm on both sides of the hot zone.

In a single pass through the furnace the fibers are heated to the peak temperature in 4-8 minutes, dwell at the peak temperature for 1-2 minutes, and are cooled at the same rate as they are pushed out of the hot zone. Most experiments involve multiple passes in an effort to induce directional recrystallization (see Section 3.2). Figure 2.9 is an example of the temperature time record of an experiment with three passes. The minimum temperature between successive passes depends upon when the motor direction is manually reversed, but is always below 750°C. After sintering the

---

3. Microstrate<sup>TM</sup> ceramic substrate, Ceramic Process Systems Corporation

4. "Moldatherm" furnace insulation board, Lindberg -A Unit of General Signal Corporation, Chicago, Illinois

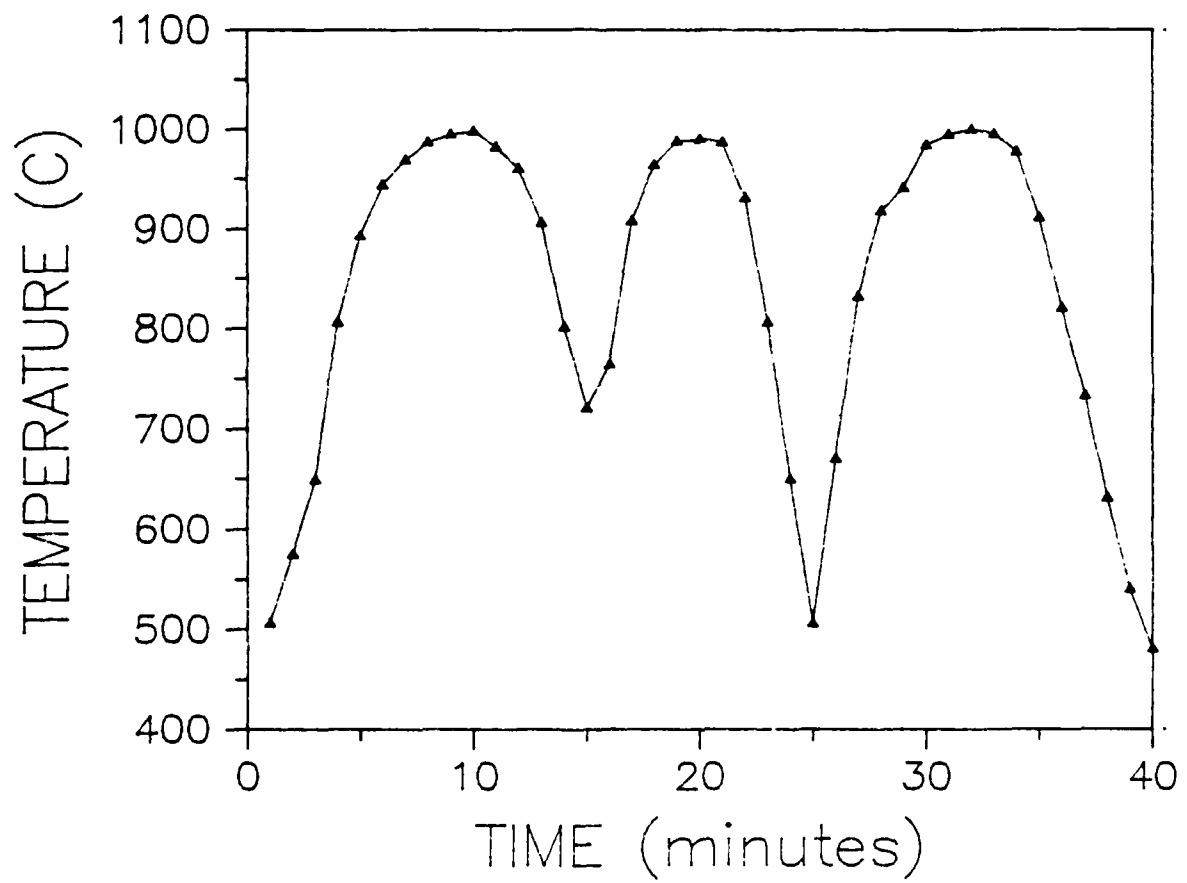


Figure 2.9 Temperature - Time Record for a Zone Sintering Experiment

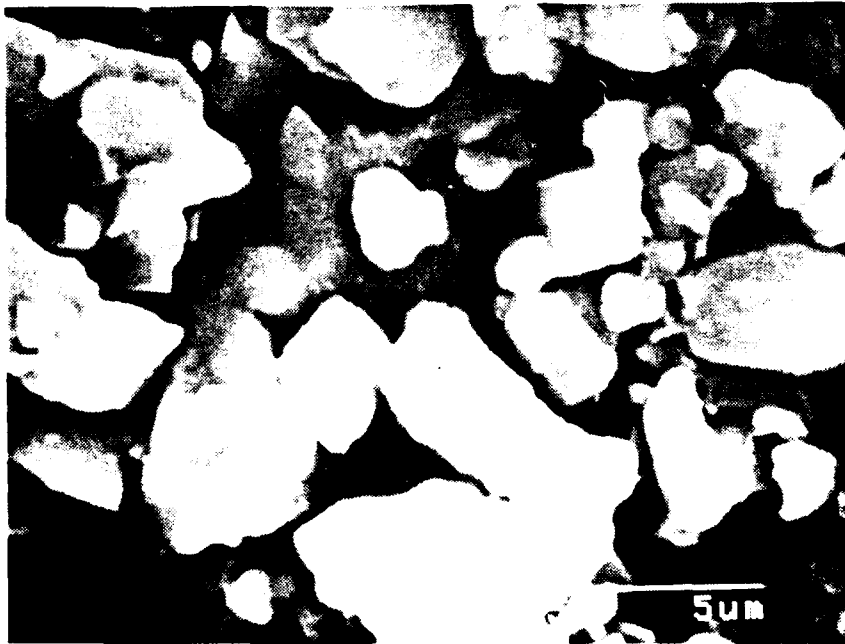
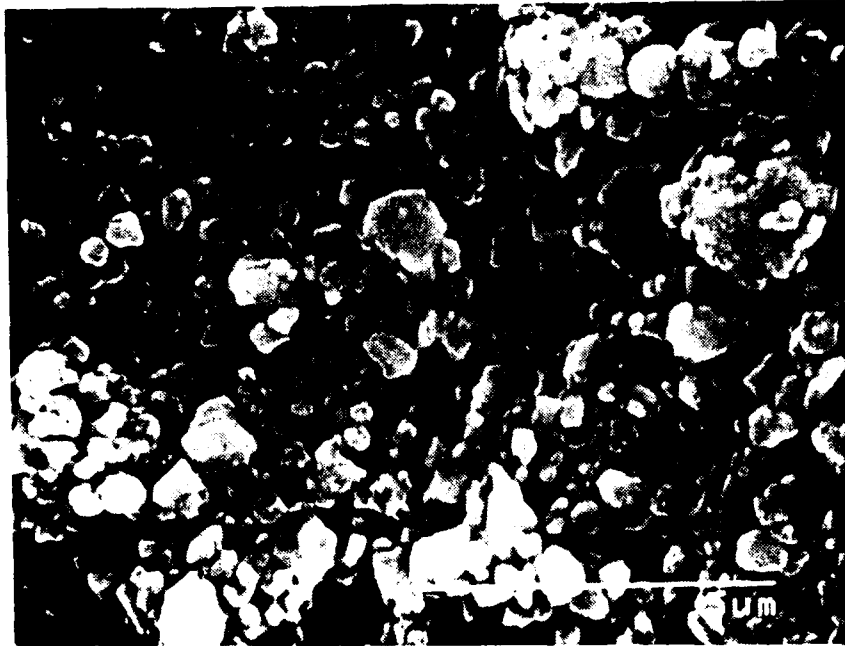


Figure 2.10  $\text{YBa}_2\text{Cu}_3\text{O}_{7-x}$  Particles in Green Fiber after Binder Burnout  
Above: Fiber 24434, Dry Vibromilled Powder  
Below: Fiber 26809, Cyclohexane Milled Powder 10,000X

fibers are presumed to be in the tetragonal phase. The sintered fibers are examined in the microscope to estimate their density and observe the grain morphology. Some fibers are exposed to an oxygen intercalation anneal at 500°C for twelve hours. These annealed fibers are presumed to be orthorhombic, since they display a Meissner Effect by levitation and exhibit characteristic twinning in the polarizing microscope.

Most fiber zone sintering experiments are conducted with green fiber, and binder burnout occurs during the rapid heat up in air as the fiber is pushed into the furnace. This is usually satisfactory. In these cases binder removal appears to occur gradually, with no visually noticeable smoke formation. However, in some cases with larger diameter fibers, combustion occurs, and a combustion zone can be seen propagating along the fiber, rather like the flame on a fuse. This causes the fiber to break up into small pieces about 1 mm long. This problem can be avoided by heating the fiber in an oxygen-lean environment to suppress combustion. Several experiments have been done in which the fibers are heated to 400°C in nitrogen or nitrogen-5% oxygen, followed by heating to 500-600°C in oxygen or air. The sintering behavior does not seem to be sensitive to the binder removal treatment, although no systematic study has been done. The design of the continuous sintering furnace will incorporate a burnout zone in which most of the binder can be removed in an oxygen-lean atmosphere.

Three lots of  $\text{YBa}_2\text{Cu}_3\text{O}_{7-x}$  fiber have been examined up to this point. The early work involved fibers spun from a powder which had been dry vibromilled. The fibers designated 24434 were prepared using powder dry vibromilled to produce a specific surface area of  $12.5 \text{ m}^2/\text{gm}$  (This is the

same dry milled powder discussed in Section 2.2.2) The fibers 24484 were made from a similar dry vibromilled powder. Recently we have begun to make fibers from the powder milled in cyclohexane for 4.5 hours, designated 26801. This is the powder whose pellet sintering behavior was shown in Figure 2.6. It is similar to as-calcined powder, with the cyclohexane milling serving to remove the larger agglomerates. At present, we have sintering data only on the CuO-doped version of these fibers, designated 26808. The static sintering behavior of this fiber has been shown in Figure 2.7. The surface area of the powder in this series of fibers is much lower, around  $0.6\text{m}^2/\text{gm}$ , but they are highly sinterable due to the addition of the 5 wt% CuO sintering aid. The  $\text{YBa}_2\text{Cu}_3\text{O}_{7-x}$  particles in both types of fibers are compared in Figure 2.10, showing fibers 24423 and 26809 after binder burnout. The extended dry vibromilling produced particles in the range of 0.1-1.0 microns, while after the shorter wet vibromilling the particle size ranged between 1 and 4 microns.

Fibers from the finer powder begin to display appreciable densification after several passes at a peak temperature of  $898^\circ\text{C}$  where it achieves about 85% density, as estimated by a point count on a fracture surface. A single pass to a peak temperature of  $918^\circ\text{C}$  yields a density around 90%. Four passes produce a density around 93% at  $938$  and  $953^\circ\text{C}$  and around 98% at a peak temperature of  $989^\circ\text{C}$ .

Figure 2.11 shows the evolution of the microstructure of the undoped fiber 24434, prepared from the dry vibromilled powder. For this experiment the fiber was passed at 5.5 cm/minute through a furnace with a peak temperature of  $998^\circ\text{C}$ . On each pass the fiber spends less than one minute at the peak temperature, and 3 minutes above  $985^\circ\text{C}$ . Significant sintering

occurred during the first pass, shown of the upper right in Figure 2.11. A second pass causes further densification and more than a doubling of the size of the grains at the surface, as shown on the upper left. The actual grain size, however, is much larger than is apparent from the surface. Figure 2.12 is a fracture surface showing the cross-section of the two-pass fiber adjacent to the surface. Large grains, 5-10 microns in long dimension, are common. The remaining pores are mostly isolated spherical pores entrapped within grains. It is difficult to estimate density accurately from fracture surfaces, but this fiber seems to be around 99% theoretical density.

The as-fired and fracture surfaces of another fiber exposed to three passes at 6.2 cm/minute with a 998°C peak temperature are compared in Figure 2.13. The fracture surface shows apparently randomly oriented grains larger than 20 microns resulting from an extensive recrystallization. About 2 volume percent residual pores and small pockets of smaller grains are visible in this micrograph. The as-fired surface seems to have a slight texture, with numerous grains aligned approximately along the fiber axis, which is horizontal in the figure. Many of these grains may be "ghosts" since the actual grain size seen in the interior is much larger than the apparent surface grain size. The texture is more clearly seen in the optical micrographs presented in Section 3.

The CuO-doped fibers from lot 28609 densified in the same temperature range, but produced much larger grain sizes due to the larger starting particle size and presence of additional liquid phase sintering aid. Figure 2.14 shows the cross section of a CuO-doped fiber which had experienced two passes at 4.5 cm/minute with a peak temperature of 989°C.



After ten passes at this temperature, the fiber surface displayed very distinct tabular grains, as shown in Figure 2.15.

A few experiments were done in which the fibers were isothermal presintered by holding them in the hot zone statically, followed by zone sintering. This was to try to separate the densification process from the attempted directional recrystallization. An isothermal hold for 37 minutes at 925°C only partially densified the CuO-doped fiber. Figure 2.16A is a cross-section of the presintered fiber, which appears to be only 84% dense by a point count. Subsequently exposing this fiber to six passes at 4 cm/minute to a 971°C peak temperature results in the structure shown in Figure 2.16B. The zone sintering has increased the density, and caused recrystallization. Figures 2.17 A and B show the fracture and as-fired surface of a fiber with a more extensive isothermal pretreatment of two hours at 950°C, followed by six passes at 971°C peak temperature. The isothermal treatment itself caused full densification and significant grain growth, with more extensive recrystallization occurring during the zone sintering. Often a single grain would extend through the cross section, as shown in Figure 2.17A. The as-fired surface, Figure 2.17B seems to show a preference for grains running oblique to the fiber axis. This is discussed in more detail in Section 3.

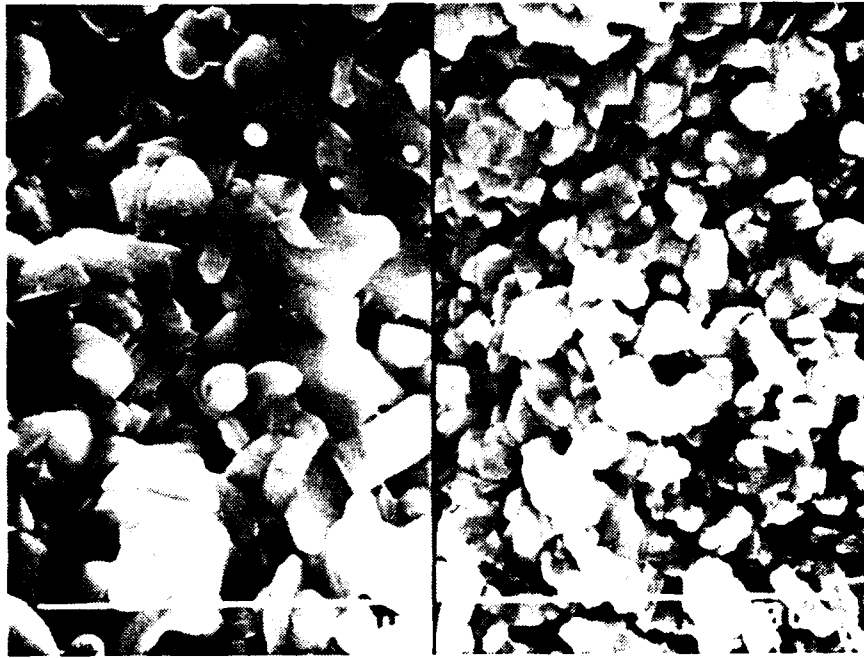


Figure 2.11 Surface of Undoped Fiber 24434 Zone Sintered at 998°C  
Right: one pass Left: two passes 5000X

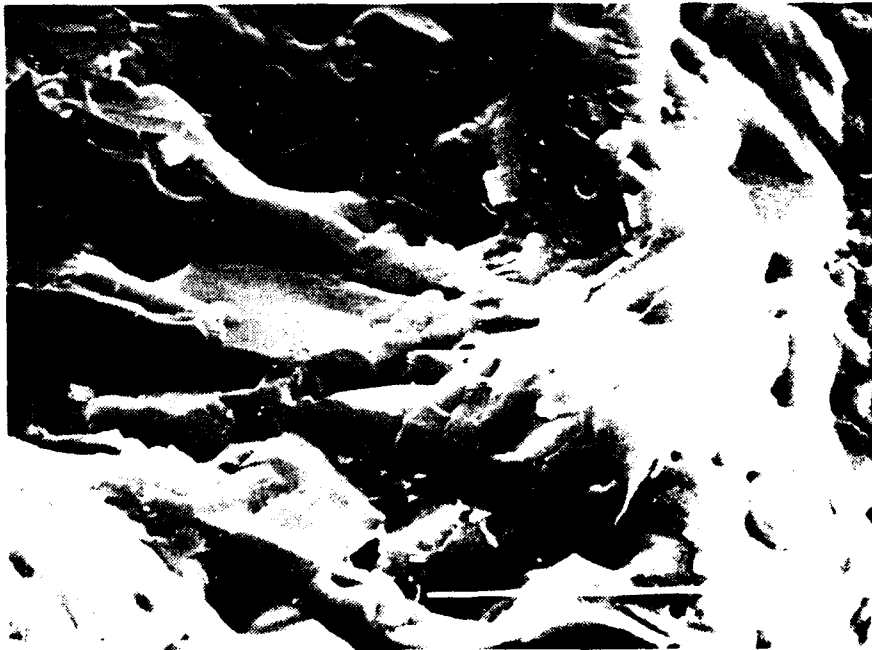


Figure 2.12 Fracture Surface of Undoped Fiber 24434 After  
Two Passes at 998°C 5000X

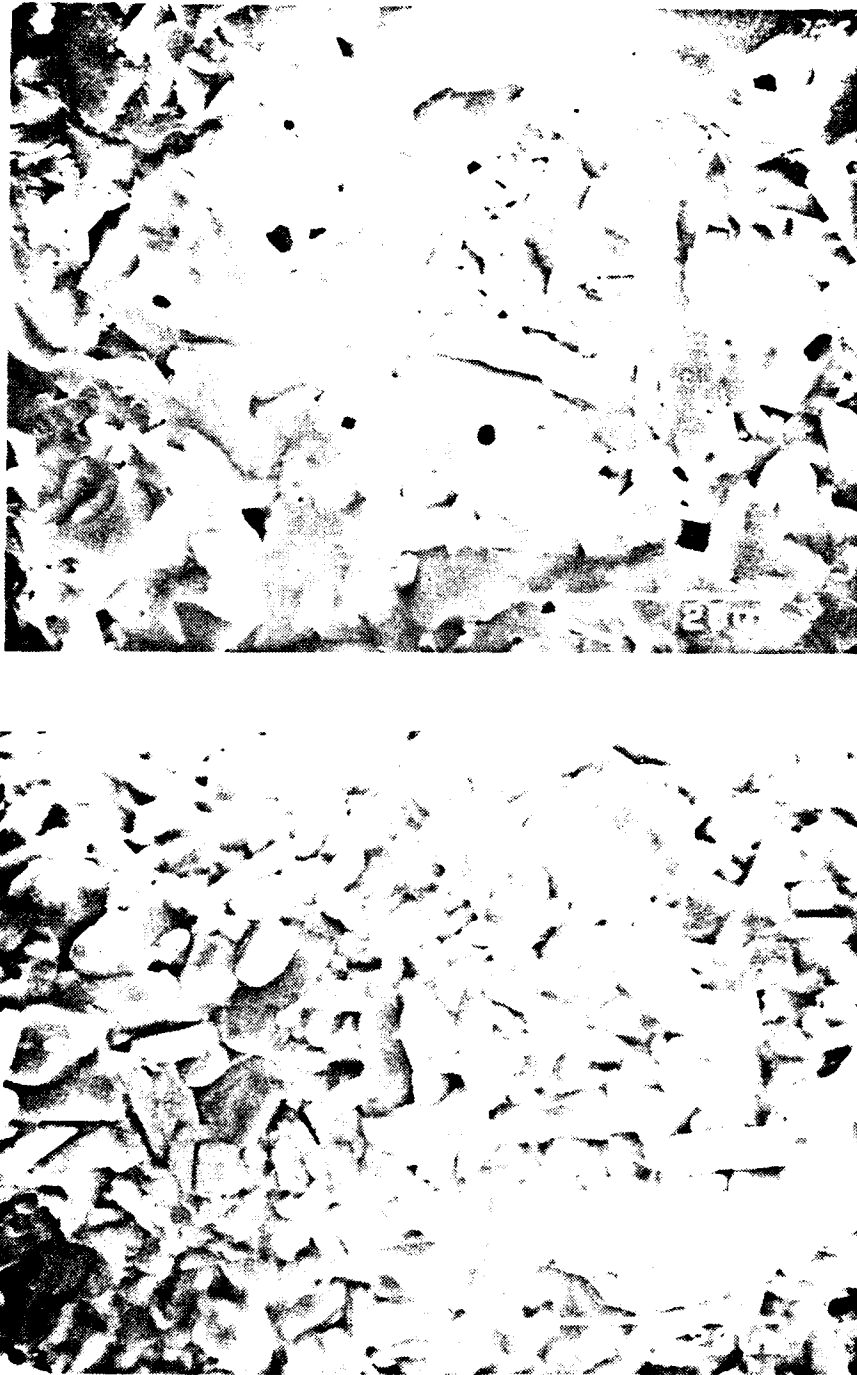


Figure 2.13 Undoped Fiber 24434 Zone Sintered for Three Passes  
At 998°C Above: Cross-section Below: Surface  
2000X

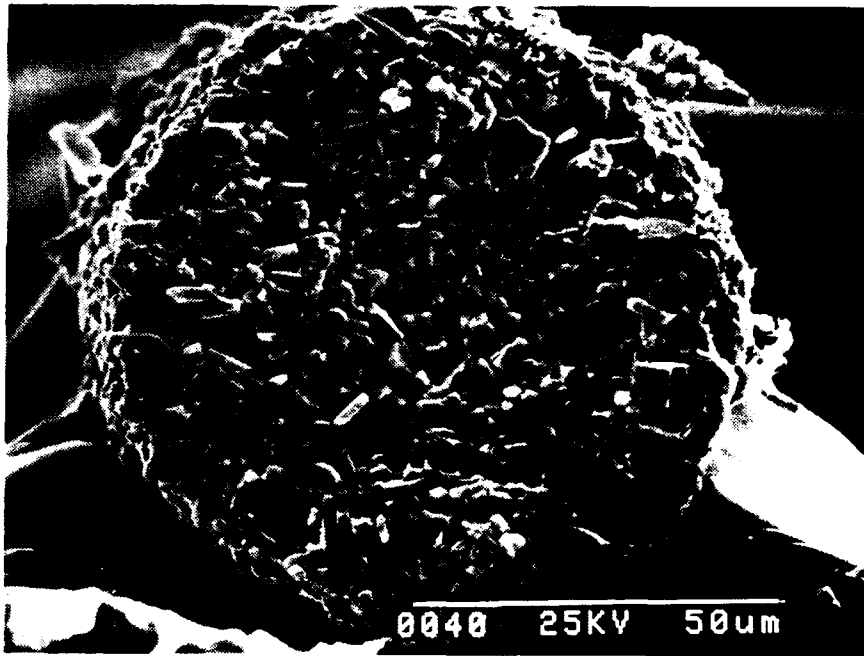


Figure 2.14 Fracture Surface of CuO-Doped Specimen 24950B  
Zone Sintered for Two Passes at 989°C  
1000X



Figure 2.15      Surface of CuO-Doped Fiber after Ten Zone  
Sintering Passes at 989°C      Specimen 24950C  
2000X

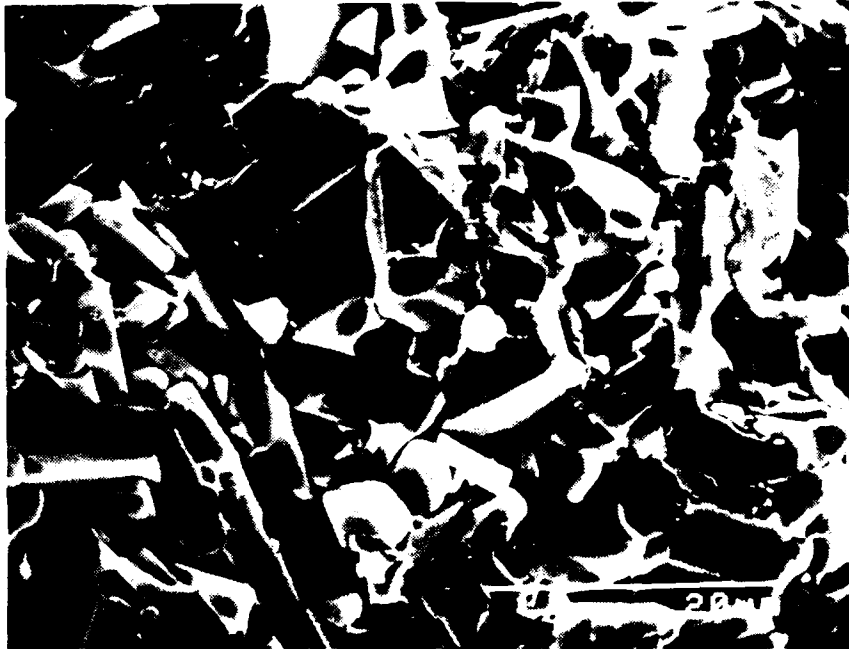


Figure 2.16A CuO-Doped Fiber Presintered 37 Minutes at 925°C  
2000X

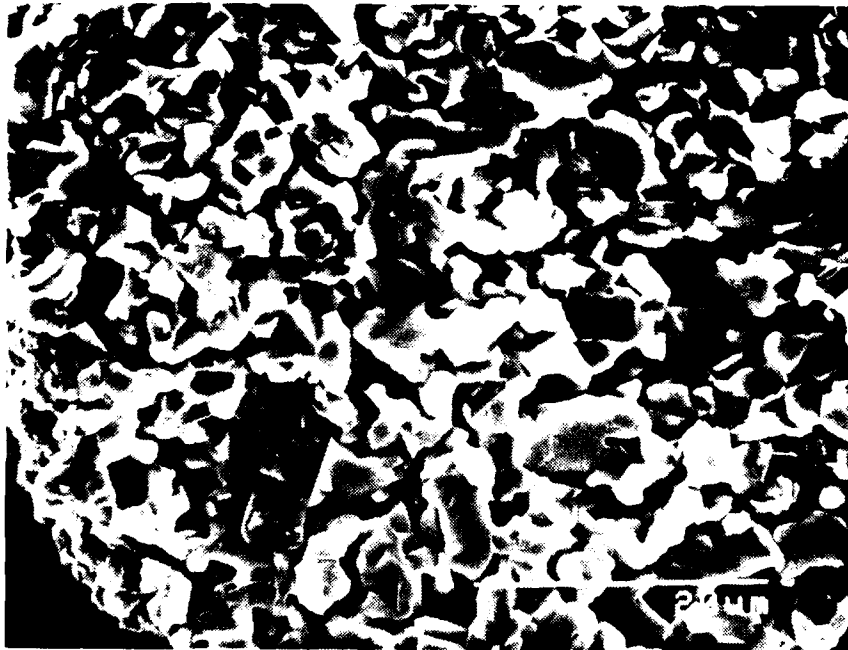


Figure 2.16B CuO-Doped Fiber Presintered 37 Minutes at 925°C  
and Zone Sintered for Six Passes at 971°C  
2000X



Figure 2.17A Cross-Section of CuO-Doped Fiber Presintered Two Hours at 950°C and Zone Sintered for Six Passes at 971°C 2000X



Figure 2.17B Surface of CuO-Doped Fiber Presintered Two  
Hours at 950°C and Zone Sintered for Six Passes  
at 971°C 2000X



#### 2.2.4 Compatibility Test

It will probably be necessary to support the  $\text{YBa}_2\text{Cu}_3\text{O}_{7-x}$  fibers during sintering by laying them on a moving furnace belt or by braiding them with a support wire or refractory fiber. The compatibility of the  $\text{YBa}_2\text{Cu}_3\text{O}_{7-x}$  with the support material is a very important issue. It is unlikely that any useful materials will be truly inert, but the very brief sintering process may permit the use of otherwise reactive materials, provided there is negligible interaction. We have observed that no apparent reaction occurs between the  $\text{YBa}_2\text{Cu}_3\text{O}_{7-x}$  fibers and the alumina substrates during the zone sintering experiments at temperatures below  $1000^\circ\text{C}$ . Above that temperature, or after long periods at lower temperature, the fibers react, staining the alumina and often causing the fiber to stick to the substrate. Hence alumina seems an acceptable support material only for rapid sintering cycles.

The  $\text{YBa}_2\text{Cu}_3\text{O}_{7-x}$  also seems to be relatively unreactive with refractory metal alloys such as Chromel and Alumel. For example, small pieces of 255 micron diameter (30 gauge) chromel and alumel wires<sup>5</sup> were buried in crucibles packed with  $\text{YBa}_2\text{Cu}_3\text{O}_{7-x}$  powder and annealed in air for 14 hours at  $950^\circ\text{C}$ . After this relatively severe treatment, both wires retained usable strength and flexibility. Metallographic examination of the chromel wire showed about a 10 micro thick reaction zone in the alloy, with about 25 microns of an adherent scale. The alumel was more reactive, having a 25-50 micron thick reaction zone in the alloy and a thick 100 micron scale.

---

<sup>5</sup>. Alloy CH and Alloy A, Nanmac Corporation, Framingham, MA

However, it seems that both alloys could be suitable for use as carrier wire braided with  $\text{YBa}_2\text{Cu}_3\text{O}_{7-x}$  fiber.

To examine reactivity during actual zone sintering conditions, samples of undoped fiber (24484) and CuO-doped fiber (26809) were placed on a variety of materials and exposed to four passes through the zone sintering furnace at typical sintering conditions of  $974^\circ\text{C}$  at 5.3 cm/minute. The two fibers were placed on an alumina rigidized fiber board<sup>6</sup>, a woven fabric of refractory alumina-silica-boria fiber<sup>7</sup>, an as-ground surface of magnesia partially stabilized zirconia ceramic<sup>8</sup>, and were placed inside small coils wound from chromel wire. After the four passes at  $974^\circ\text{C}$ , which were sufficient to sinter both types of  $\text{YBa}_2\text{Cu}_3\text{O}_{7-x}$  fiber, none of these materials displayed any visual evidence of reaction. There was no sticking, discoloration, or staining of the  $\text{YBa}_2\text{Cu}_3\text{O}_{7-x}$  or the substrate materials. While this quick test is hardly definitive, it does suggest that carrier material compatibility will probably not be a problem.

---

6. Moldatherm, Lindberg-A Unit of General Signal Corporation, Chicago, IL

7. Nextel 312, 3M Company, Ceramic Materials Department, St. Paul, MN

8. Nilcra TS - MgPSZ, Nilcra Ceramics (USA), Elmhurst, IL

### SECTION 3

#### MICROSTRUCTURAL TEXTURE

##### 3.1 Green Texture

Up to this time we have not been able to produce an adequate quantity of suitable green  $\text{YBa}_2\text{Cu}_3\text{O}_{7-x}$  fibers to examine their texture with an X-ray diffractometer. Moreover, we have focussed our energies on the production of the fiber itself, and delayed examination of the texture for later work. Very recently, however, we have been able to produce the necessary amount of straight green fiber to be able to make a large enough bundle of aligned fibers to examine on the diffractometer, and are now very actively working on characterizing and enhancing particle texture in the fibers.

We expect to be able to generate a strong preferred particle orientation in our green fibers. Fiber spinning involves extensive elongational flow as the fiber is attenuated below the spinnerette. In our cases, the ultimate fiber diameter is often 10-20 times smaller than the spinnerette diameter (see Section 4). A unit volume is thus elongated by a factor of 100-400 times along the axial direction. It seems plausible that non-axisymmetric particles will be strongly aligned by this stretching process. Moreover, the elongational flow continues until the fiber is effectively frozen by the increased viscosity caused by loss of solvent. This should serve to fix the orientation state created by the elongational flow. The key will be producing  $\text{YBa}_2\text{Cu}_3\text{O}_{7-x}$  particles with an

appropriately platey habit. As illustrated by Figure 2.1A, the primary  $\text{YBa}_2\text{Cu}_3\text{O}_{7-x}$  particles produced by our calcination are adequately platey. Unfortunately they are strongly agglomerated. Up to the present we have not found a suitable milling condition to liberate these platey particles. We have either milled too long, and ground them into equiaxed micron-sized fragments, or milled so briefly that the particles were still agglomerated. Currently we have underway a series of experiments which will identify the milling conditions which produce a high yield of platey particles. These particles will be incorporated into fibers, and the texture will be assessed by examining the relative intensities of the (006), (020), and (002) family of diffraction lines. Fibers will be sintered isothermal to determine the extent to which the texture is changed by sintering and recrystallization.

### 3.2 Directional Recrystallization Experiments

One of the strategies for production of a textured microstructure is "directional recrystallization". The concept is to exploit the tendency of  $\text{YBa}_2\text{Cu}_3\text{O}_{7-x}$  to develop grains having a platey habit with the  $\langle 001 \rangle$  axis normal to the habit plane. It is likely that this habit develops during liquid phase sintering because grain growth is more rapid along the  $\langle 010 \rangle$  directions. This suggests that a strong texture can be produced by controlling this grain growth with a gradient to force a directional recrystallization. For continuous fiber sintering, directional recrystallization could be promoted by controlling axial temperature zones in the furnace. For example, passing the sintered fiber through zones alternately hotter and cooler than the solidus temperature, may propagate a

"wave" of CuO-rich liquid down the fiber axis. Multiple passes may have the effect of propagating recrystallization fronts along the fiber axis. This should allow a controlled amount of texture to be created in the sintered fiber.

We are attempting to test this on a small scale by passing short lengths of fiber through a temperature gradient at a controlled rate. The important variables are peak temperature, temperature gradient, fiber velocity, number of passes through the gradient, and the microstructure prior to the directional recrystallization treatment. The latter is adjusted by an isothermal presintering step to establish a starting density, grain size, and shape. To search for the appropriate conditions, we simply examine the microstructure by SEM and optical microscopy. The texture is very obvious upon examination of the microstructure, so microscopy suffices for the present. For this preliminary work we are sintering only one or two pieces of fiber in each experiment, so our specimens are too small to determine their texture using an x-ray diffractometer. Each fiber specimen is about two centimeters in length, and weighs between 0.5 and 5 milligrams, depending upon fiber diameter. Experiments are planned to correlate the microstructural observations with X-ray diffraction using a Debye-Scherrer camera, which can accept our tiny specimens.

The grain texture is now being semi-quantitatively assessed using stereological methods. Polished sections of fibers are photographed through an optical microscope between crossed polars to maximize contrast between the grains. A transparent overlay is placed on the photograph and a ruler is used to draw lines parallel to each grain. This method

introduces a bias toward the more distinct grains, which have a high probability of being traced, and against the fainter grains which may be overlooked. The angles between the grain traces and the fiber axis is measured with a protractor and recorded on a histogram. The distribution of grain trace angles contains the grain orientation distribution, which is the desired information, but is convoluted with a function dependent upon the plane of polish. We believe it is possible to recover the true orientation distribution from the trace angle data, but we have not yet solved the stereological problem. The raw trace angle data will have to suffice for the present.

Figure 3.1 is the polished section of an undoped fiber 24434 after three passes at a peak temperature of  $998^{\circ}\text{C}$ , taken with crossed polars at  $400\times$ . The traces of thin platy grains are visible, some stretching almost half the distance across this 200 micron diameter fiber. The average size of these platy grains was determined by point count to be 15 microns long and 2 microns thick. A  $\text{CuO}$ -doped 28609 fiber is shown in Figure 3.2, taken at the same magnification. Distinct grains, chosen for measurement by a random point count, had an average length of 10 microns and average width of 3 microns. This fiber received ten passes at  $989^{\circ}\text{C}$ , followed by an oxygen intercalation anneal. The oxygen anneal converted the material to the orthorhombic phase, as indicated by the characteristic twinning. Figure 3.3 shows the same fiber at  $1000\times$ , under contrast conditions to enhance the twin structure.

The first visual impression of these fibers is that they have a "tweed" texture, with many grains about 45 degrees to the fiber axis. This is confirmed by the stereological measurements shown in Figure 3.4.

which are histograms of the angles between the traces of the grain habit planes and the fiber axis. The CuO-doped fiber has the most striking texture, with all of the measured angles tightly clustered around a mean of 51 degrees. Almost 70% of the measured grains fell in the angle range 40-60 degrees. If the grains were randomly distributed, only 22% would be expected in this range. In the range 30-70 degrees, a random distribution would have 44%, but this fiber had 96% of its grains intersecting the fiber axis in this range of angles. The undoped fiber 24434 also has a less pronounced but still non-random distribution, with 36% in the 40-60 range, and 70% in the 30-70 range. The histogram for this fiber may be bimodal.

We do not understand what causes this apparent tweed texture. Upon close examination of SEM micrographs, one can find a number of chevron-shaped features which are possible growth twins<sup>9</sup>. (See Figures 2.15, 2.16, and 2.17). If secondary grains tend to form growth twins during recrystallization, a tweed texture may be enhanced. It is not clear what process creates the near-45 degree orientation during our directional recrystallization experiments. Further work is underway.

A further means of inducing a texture is simply to permit very extensive recrystallization so that the grain size exceeds the fiber diameter. As this occurs, grains oriented at large angles with the fiber axis will impinge on the fiber surface and stop growing. Grains oriented at small angles to the fiber axis can continue to grow, propagating down the fiber axis and consuming the smaller grains. This would create fibers

---

<sup>9</sup>. A growth twin would form during recrystallization of the tetragonal phase during sintering. It should not be confused with the transformation twins formed in by the tetragonal-to-orthorhombic transformation.

consisting of only a few grains in cross-section. The isothermal sintered CuO-doped fibers, shown in Figure 2.7, show evidence of this process in an early stage. An optical micrograph of this fiber appears in Figure 3.5, showing a 200 micron long grain running down the length of a 100 micron diameter fiber. Presumably a longer anneal would have produced a greater population of these grains. This process could also be enhanced by decreasing fiber diameter, so less grain growth is required. As a practical matter, monofilament fiber smaller than 30 microns are very difficult to handle. To use very fine diameters, it is convenient to spin multifilament green fibers. We are investigating multifilament dry spinning.



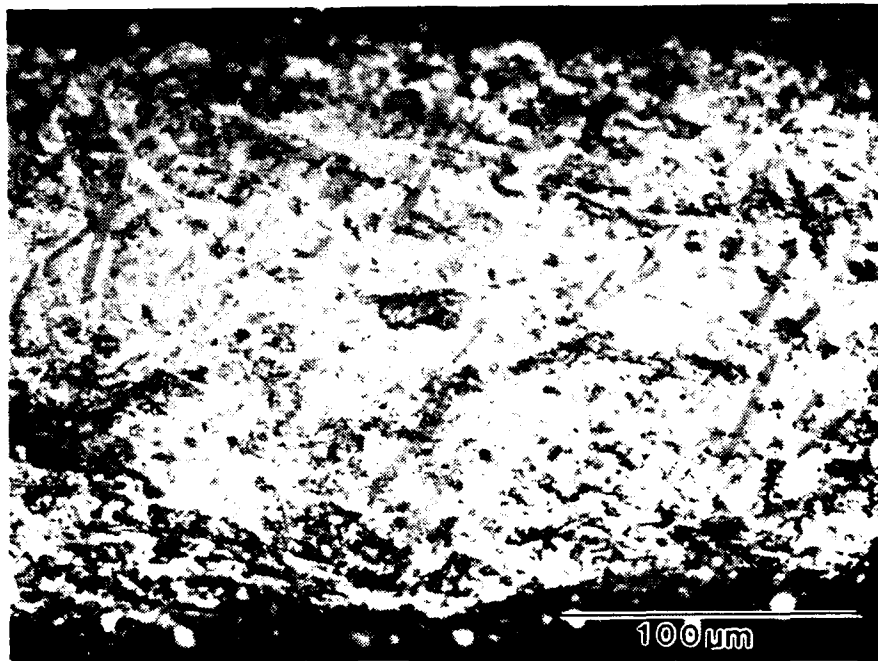


Figure 3.1 Polished Section of Undoped Fiber 24434 Zone  
Sintered for Three Passes at 998°C  
crossed polars 400X

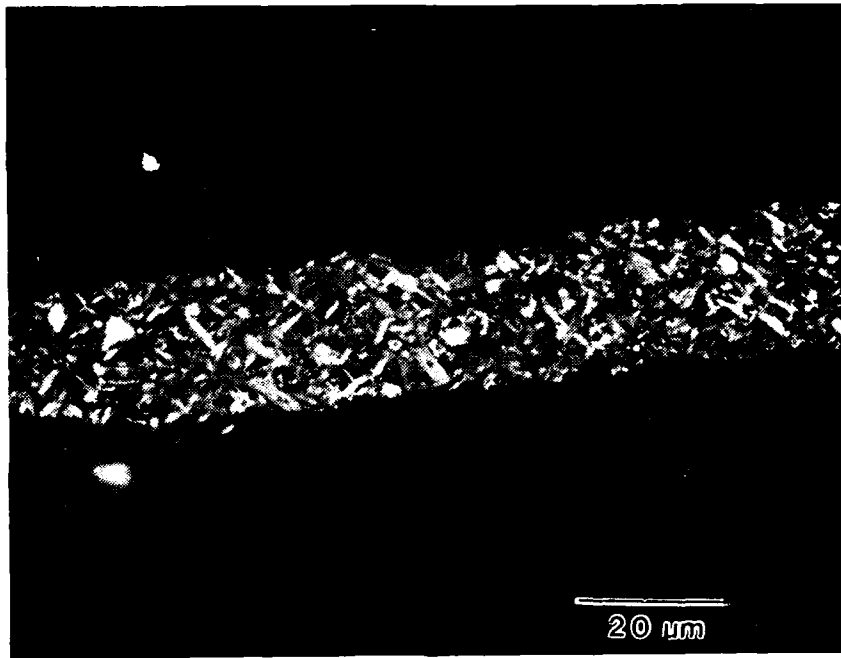


Figure 3.2 Polished Section of CuO-Doped Fiber Zone Sintered  
Ten Passes at 989°C and Oxygen Annealed at 500°C  
crossed polars 400X

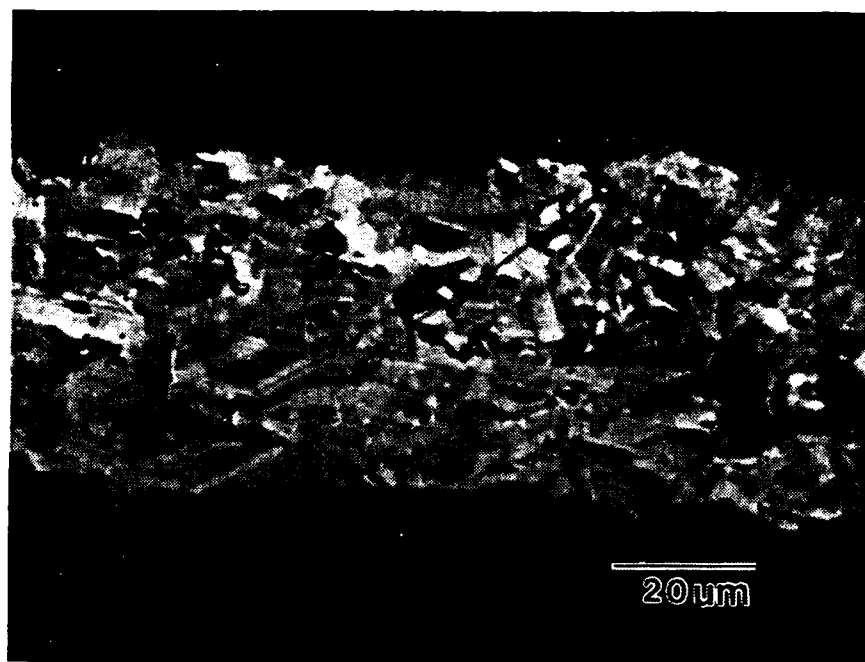


Figure 3.3      Twinning in CuO-Doped Fiber Zone Sintered  
Ten Passes at 989°C and Oxygen Annealed at 500°C  
crossed polars      1000X

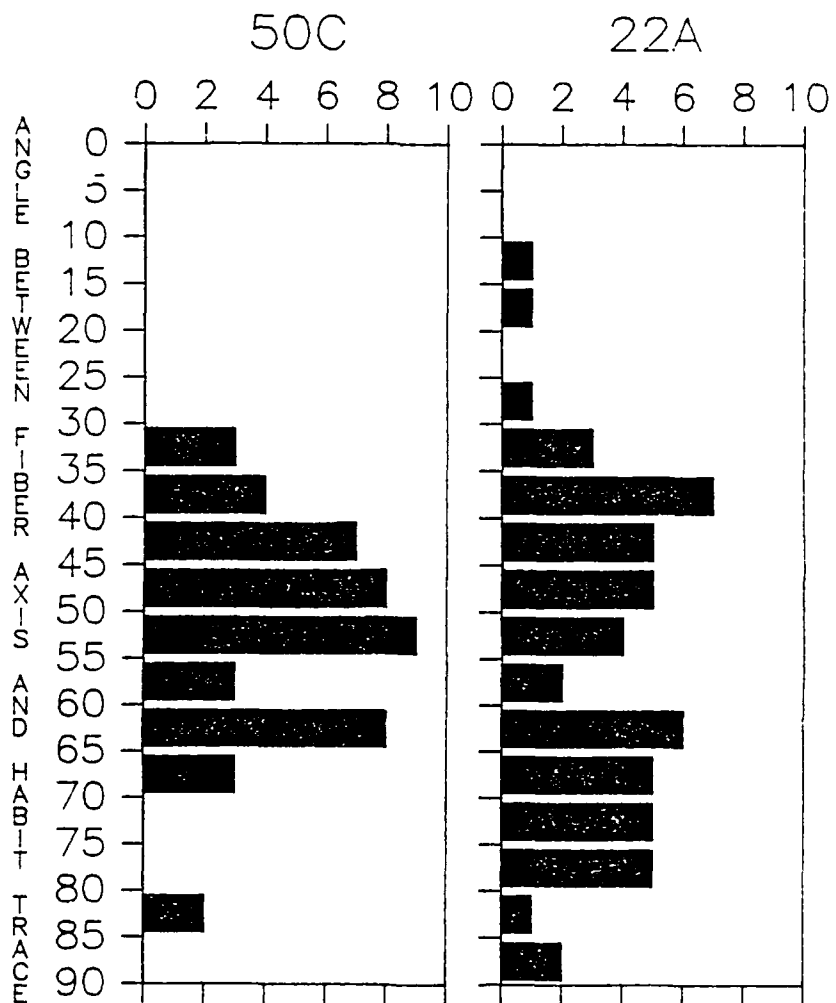


Figure 3.4 Distributions of Measured Angles between Fiber Axis and Traces of Grain Habit Planes for a CuO-Doped 26809 Fiber (Specimen 50C) and Undoped 24434 Fiber (Specimen 22A)

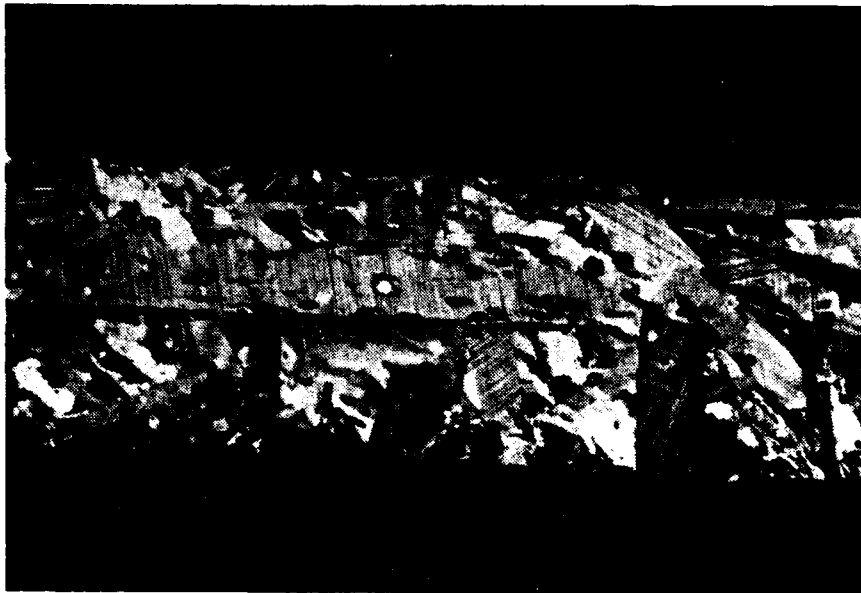


Figure 3.5 Polished Section of CuO-Doped Fiber Sintered  
Isothermally for 15 hours at 965°C  
crossed polars 400X

## SECTION 4

### ELECTRICAL MEASUREMENTS

Electrical resistivity measurements were made on specimens cut from sintered pellets made with undoped powder A (see Section 2.2.2). These pellets were sintered in flowing oxygen 15 hours at 998°C to 94% theoretical density or at 965°C to 75% theoretical density, cooled 5°C/minute to 500°C, where they were held for two hours before rapid cooling to room temperature. Figure 4.1 shows that the microstructure of the 94% dense specimen consists of interlocked tabular grains chiefly larger than 100 microns. Residual porosity consists mostly of spherical intragranular pores. Bars were diamond cut to approximate dimensions 10x2x2mm and electroded with silver paint to provide a four-point contact.

For these tests a Micronta DC power supply was used as a constant current source and a Kiethly 617 electrometer was used to measure the sample voltage. Temperature was measured with a Fluke 51 thermometer, using a small type K thermometer placed on the sample. The specimen was cooled by immersion in a dewar of liquid nitrogen. Specimen currents ranged from 100 to 300 milliamps. At room temperature the V-I characteristics of the specimens in the four-point configuration were ohmic. Contact resistance of the current electrodes was approximately 100 microohms. For this experiment, temperature and resistance were recorded at one second intervals during heating and cooling. "Zero" resistance was recorded when the measured resistivity fell below the resolution of the apparatus, around 20 microohm-cm.

Resistivity vs. temperature data is displayed in Figure 4.2. Room temperature resistivity ranged between 4.5 and 5 milliohm-cm for the 75% dense specimen upon repeated measurements. Resistivity decreased gradually with temperature to about 3 milliohm-cm at 100°K. For this 75% dense specimen, the superconductive transition began at 97°K and was complete around 94°K. The 94% dense specimen had a much lower room temperature resistivity, around 2 milliohm-cm, and dropped gradually with temperature to about 0.7 milliohm-cm at 100°K. The dense specimen had a critical temperature around 88°K, significantly lower than the porous specimen. The oxygen stoichiometry data for these specimens are not yet available.

We have recently acquired improved apparatus for electrical measurements. These are a Kiethly 228 voltage/current source and a Kiethly 197 Nanovoltmeter, with which we will improve our measurements. Most effort at present is devoted to developing techniques for critical current measurements, for both pellets and sintered fiber. For pellets we are experimenting with specimen holders which can provide a large contact area for current leads, while keeping a small cross-section specimen. For fibers we are experimenting with specimen holders which can support and make contact with fragile sintered fibers as small as 50 microns in diameter. At present we are trying to use unclad fiber, to which electrical contact will be made with silver paint applied to a relatively long region of the fiber. We expect data by the next report period. The Janus cryostat for controlled temperature work has not yet been delivered.

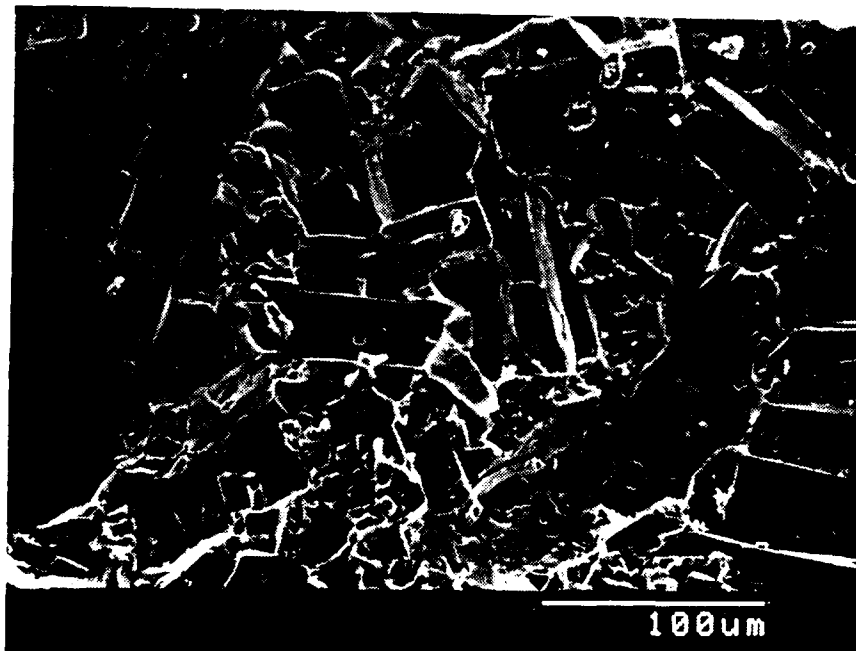


Figure 4.1 Fracture Surface of the 94% Dense Undoped Specimen  
Used for Resistivity Measurements  
300X



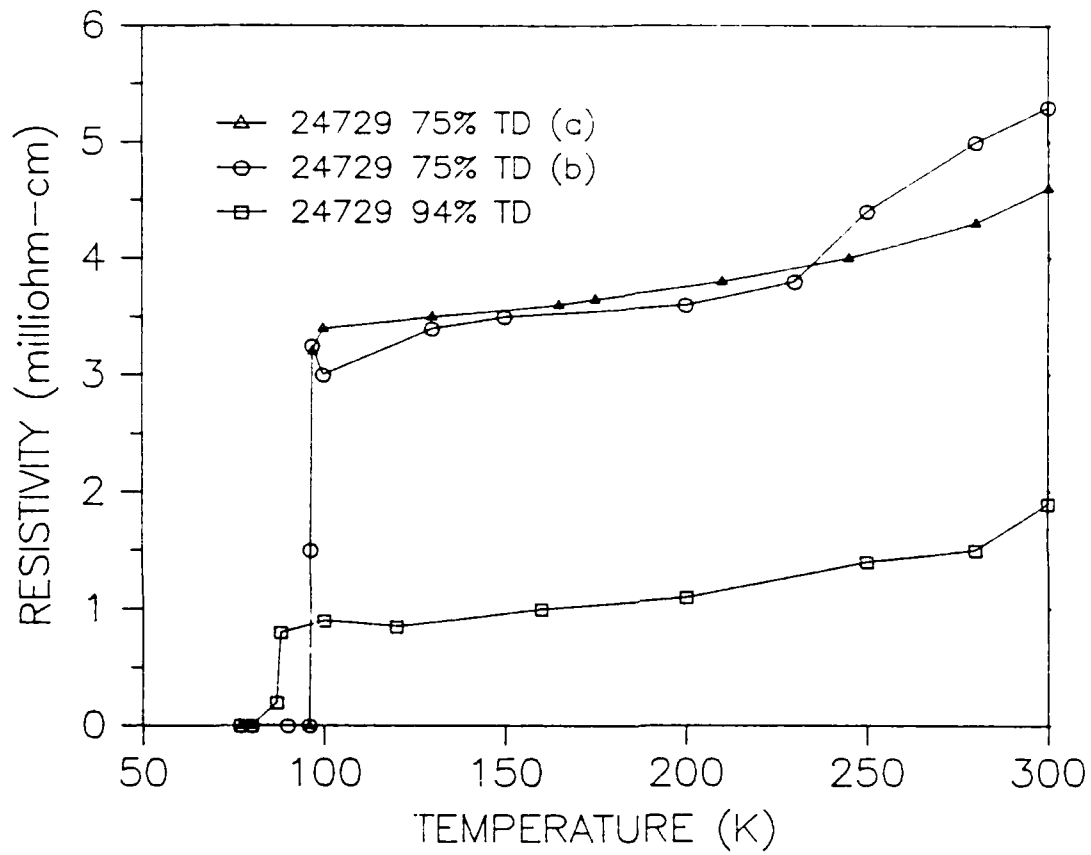


Figure 4.2 Resistivity vs. Temperature for Undoped Pellets at 75% and 94% Theoretical Density

## SECTION 5

## FIBER SPINNING DEVELOPMENT

## 5.1 Fiber Spinning Developments

During this report period research was focussed on producing  $\text{YBa}_2\text{Cu}_3\text{O}_{7-x}$  fibers using "standard" dry spinning formulation, investigating powder characteristics associated with good spinnability, and on efforts to develop capability to produce continuous lengths of green fiber. In the latter effort, barium titanate powder was used as a surrogate for  $\text{YBa}_2\text{Cu}_3\text{O}_{7-x}$ , allowing us to use a readily available powder for preliminary experiments. The dry spinning apparatus underwent constant modification to improve dope delivery, control the flow of drying air, and improve the drying of the fiber. At present we are able to spin continuous lengths of uniform fiber, but are unable to collect the fiber continuously on the spooler, primarily because of incomplete drying due to an inadequately long drying column. For present purposes we capture 2-3 meter lengths of fiber from the continuous stream. This is sufficient to support much of our experimental program. Figure 5.1 shows some of the fibers made in the apparatus from  $\text{YBa}_2\text{Cu}_3\text{O}_{7-x}$  and barium titanate.

Most experiments have used the standard formulation listed in Table 5.1, which is the same as discussed in the previous report. This formulation is reasonably satisfactory, so only a few experiments were devoted to improving it during this period. The plasticizer was removed in hope of increasing green strength, but we found that the properties to deteriorate as the fibers became more brittle. The crosslinking agent

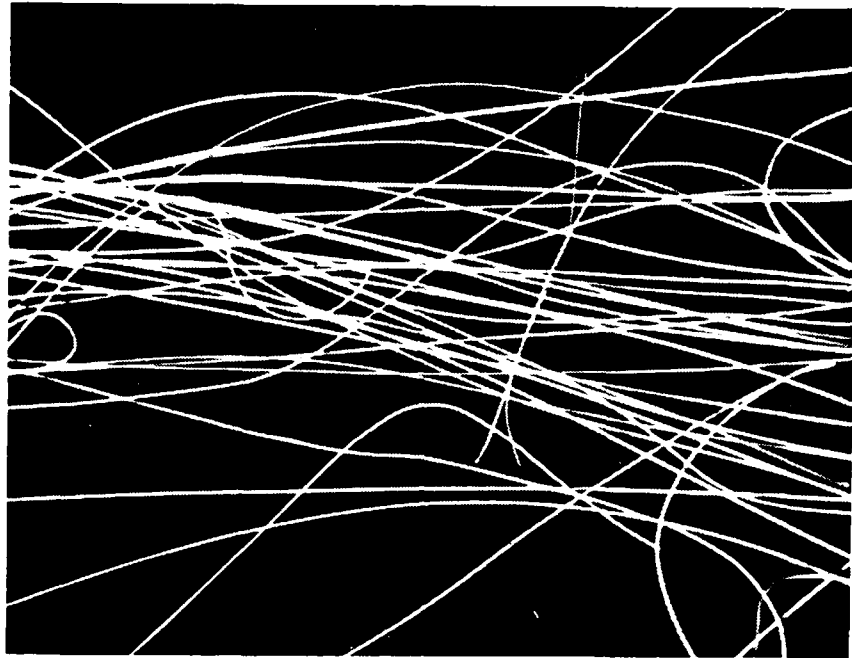


Figure 5.1 Top: Barium Titanate Green Fibers  
Bottom:  $\text{YBa}_2\text{Cu}_3\text{O}_{7-x}$  Green Fibers 6 5X

Cymel 370 had originally been added to the formulation in expectation of improved rigidity during binder burnout. In fact we never activated the crosslinking reaction between the crosslinking agent and the hydroxyl functional AT-63, as it turned out that binder burnout caused no problem. In an attempt to simplify the formulation, the Cymel 370 was eliminated. To our surprise, the viscosity decreased significantly, so the formulation was no longer spinnable. We found it more expedient to retain the Cymel, rather than reformulate to re-establish a spinnable rheology. One successful formulation change involve addition of a high molecular weight polymer, Paraloid K120N, an acrylic with one million molecular weight.<sup>10</sup> This generally improved the strength and handleability of the fibers, without degrading the spinnability. To assist in the interpretation of the role of each component, we have begun to characterize the viscoelasticity of the spinning dope. (See Section 5.4).

## 5.2 $\text{YBa}_2\text{Cu}_3\text{O}_{7-x}$ Fiber Spinning

Most of the  $\text{YBa}_2\text{Cu}_3\text{O}_{7-x}$  fibers have been produced in short lengths on a bench top set-up in which fibers are pulled from dope extruded from a syringe. This proved convenient for screening a number of formulations prepared in small lots. The same formulations can be spun continuously in the larger apparatus, and we are currently producing all of the  $\text{YBa}_2\text{Cu}_3\text{O}_{7-x}$  fibers in the continuous apparatus.

The  $\text{YBa}_2\text{Cu}_3\text{O}_{7-x}$  dope development necessarily used powders produced by the still-evolving powder synthesis methods. The earlier fibers were made

---

<sup>10</sup>. Paraloid K120N, Rohm and Haas

from dry-vibromilled powder with a large specific surface area (see Section 2) due to a significant submicron fraction. This powder had a broad size distribution and was contaminated by a small fraction of agglomerates which were difficult to disperse. Efforts were made to upgrade this powder by classifying it into three size ranges by sedimentation. Later fibers were made with  $\text{YBa}_2\text{Cu}_3\text{O}_{7-x}$  powder which was wet vibromilled in cyclohexane for 4.5 hours. Attempts were also made to classify these powders. Some characteristics of these powders were discussed in Section 2.

Formulations to make  $\text{YBa}_2\text{Cu}_3\text{O}_{7-x}$  fibers are summarized in Table 5.2. The significant differences between these formulations are the particle size distribution of the powder and the amount of time the formulations were agitated before the dope was used. Significant agglomeration on the fiber surfaces were observed for formulations 24434 and 24484, both made with dry-vibromilled powders having a significant number of submicron particles and agglomerates. Formulations 26801-7 and 26817, made from the wet-vibromilled powder, did not exhibit agglomeration. The powder from which these formulations were made had an insignificant amount of submicron particles.

The dry-vibromilled powder formulations were spinnable, but made fibers with very nonuniform diameter (see Figure 5.2). The bumpy surface is probably associated with agglomerates, either preexisting in the powder or formed by poor dispersion of submicron particles in the dope. The coarser, nonagglomerated cyclohexane milled powder made more uniform fibers. Figure 5.3 shows a fiber made from formulation 26801 and Figure 5.4 shows a fiber made from formulation 26817. Note the lack of agglomerates on the surface of the fibers and the uniformity of the fiber

diameter. Comparison of these micrographs with that in Figure 5.2 indicates that better  $\text{YBa}_2\text{Cu}_3\text{O}_{7-x}$  fibers can be made with powders having a small submicron fraction. Extended agitation of the dope is necessary to insure a good dispersion of the powder/polymer mixture.

TABLE 5-1

## STANDARD GREEN FIBER FORMULATION 24424-#1

<u>COMPONENT</u>	<u>FUNCTION</u>	<u>WEIGHT %</u>	<u>VOLUME %</u>
-			
Ceramic Powder	Powder	74.63	31.07
Toluene	Slow drying solvent	2.60	7.57
Methylethylketone	Fast drying solvent	4.52	14.17
Xylene	AT-63 Solvent	6.42	18.65
SPAN 85	Dispersant	1.60	4.24
AT-63 Polymer	Low MWt. Polymer	6.41	15.09
B-7MEK Polymer	High MWt. Polymer	1.94	4.54
Paraplex G51	Plasticizer	0.94	2.49
Cymel 370	Crosslinking Agent	0.94	2.18

Table 5.2

YBa<sub>2</sub>Cu<sub>3</sub>O<sub>7-x</sub> fiber formulations

<u>Component</u>	<u>24434</u>	<u>24484</u>	<u>26801</u>	<u>26803</u>	<u>26805</u>	<u>26807</u>	<u>26817</u>
Powder used	21496B	21455A	24492A	24492B	24492C	24492D	24492B
Wt% YBa <sub>2</sub> Cu <sub>3</sub> O <sub>7-x</sub>	77.24	74.55	77.12	76.45	76.42	75.72	74.82
Wt% Toluene	2.49	3.72	2.31	2.40	2.32	2.30	2.32
Wt% Span85	0.97	0.96	0.98	0.97	0.95	0.96	1.02
Wt% AT-63	11.66	12.72	12.88	13.43	13.14	13.50	14.84
Wt% B7MEK	6.02	6.38	5.17	5.12	5.60	5.98	5.13
Wt% ParaplexG51	0.81	0.80	0.77	0.84	0.81	0.78	0.87
Wt% Cymel 370	0.81	0.87	0.77	0.79	0.76	0.76	1.00
Vol% Powder	55.0	53.7	55.4	54.4	54.6	53.8	51.7
Agitation Time	1 hr.	18 min.	20 hrs.	20 hrs.	20 hrs.	20 hrs.	1 hr.
Agglomerates on Fiber Surface?	yes	yes	no	no	no	no	no



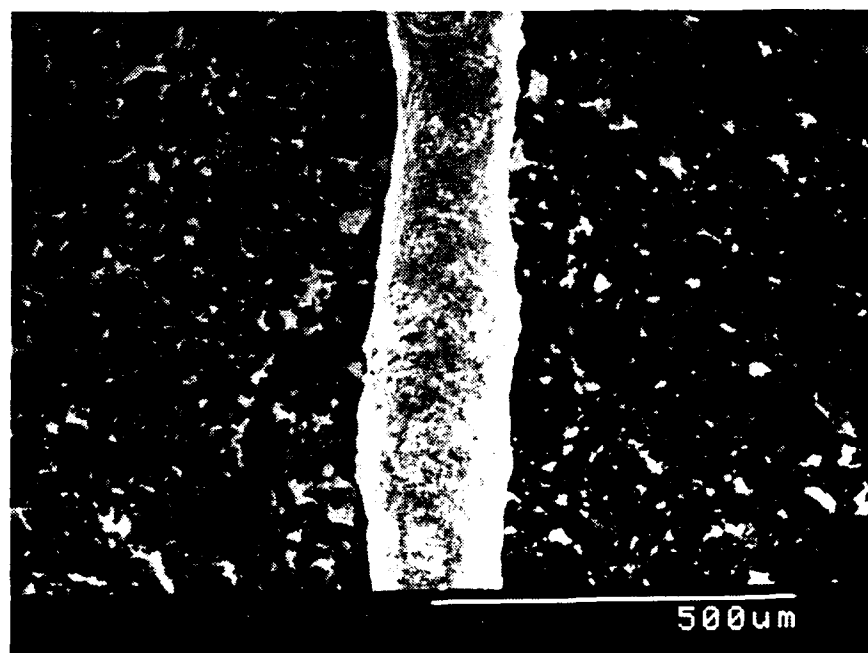


Figure 5.2 YBa<sub>2</sub>Cu<sub>3</sub>O<sub>7-x</sub> Fiber from Formulation 24484-1, Using Dry Vibromilled Powder, With Non-uniform Diameter  
100X

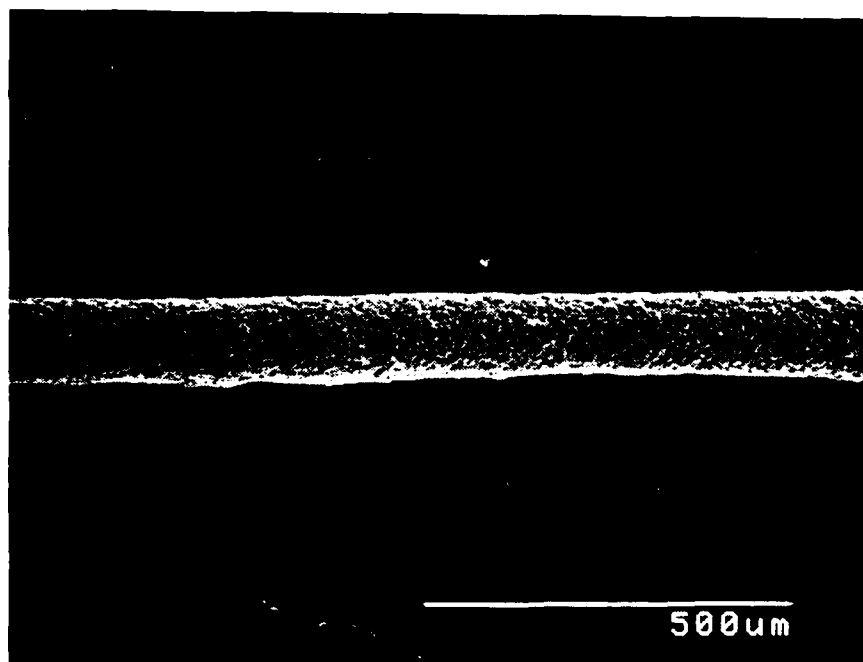
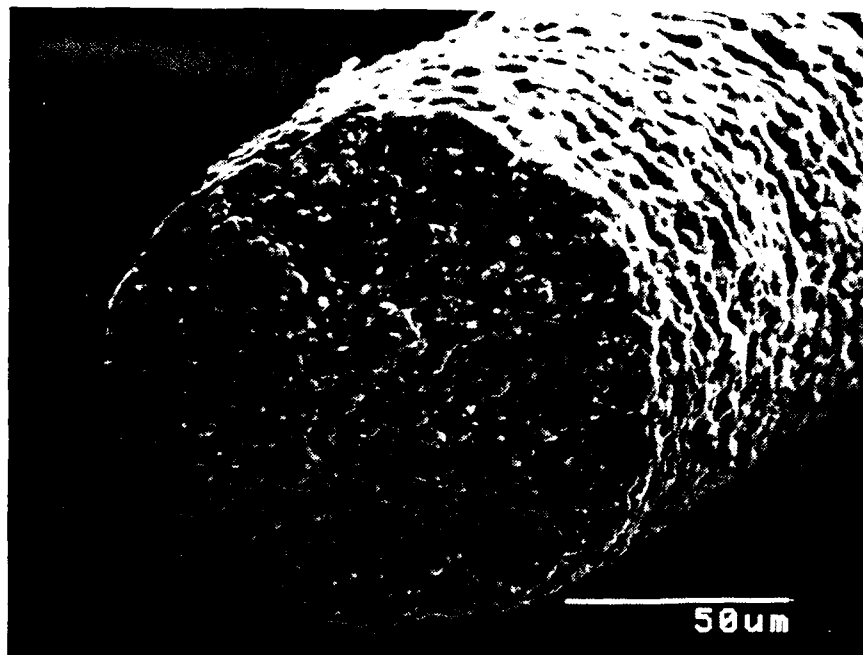


Figure 5.3

$\text{YBa}_2\text{Cu}_3\text{O}_{7-x}$  Green Fiber from Formulation 26801, Using  
Cyclohexane Vibromilled Powder  
Top: 600X      Bottom: 100X

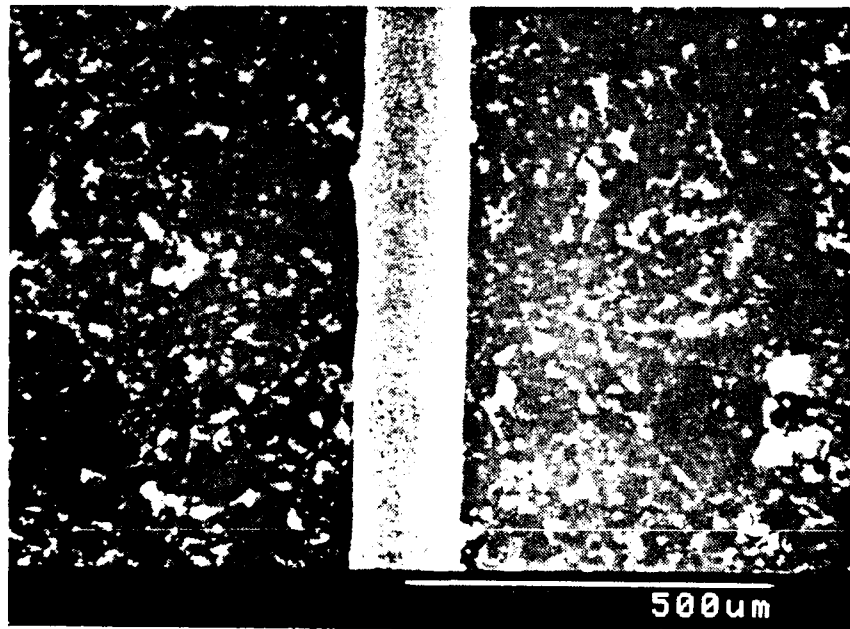
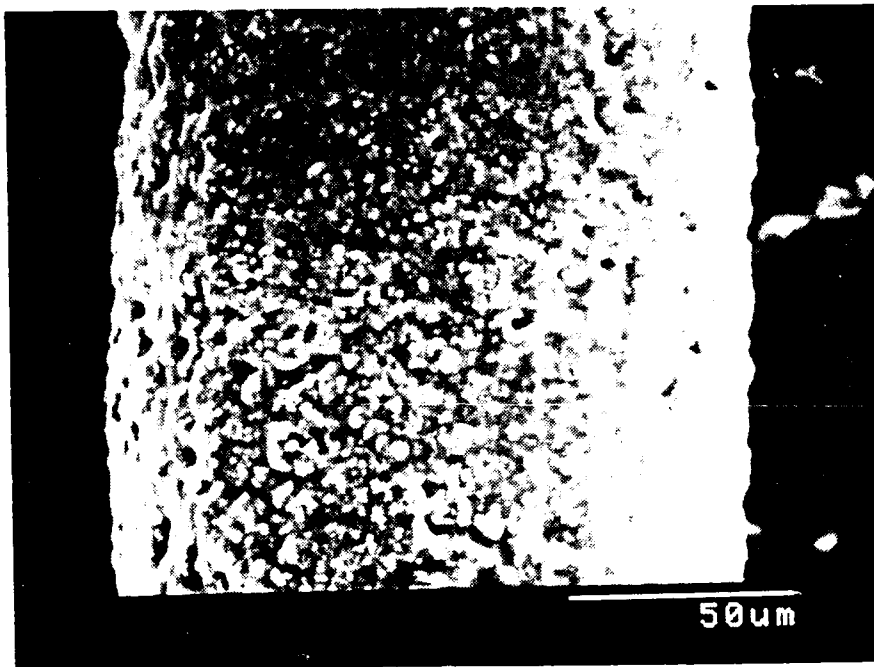


Figure 5.4  $\text{YBa}_2\text{Cu}_3\text{O}_{7-x}$  Green Fiber form Formulation 2681  
Top: 600X Bottom: 100X

### 5.3 Continuous Spinning Developments

Much of our effort this period was spent in building, re-building, and modifying the continuous fiber spinning apparatus. The spooler arrived early in this period, which motivated the increased effort, and made obvious the deficiency in the drying. In the present apparatus, the experimental slip is contained in a syringe, and extruded through disposable tips which act as the spinnerette. The dope is extruded at a rate around 0.5ml/minute either by use of a motorized syringe pump which moves the plunger at a controlled rate, or pneumatically by adjusting pressurized air on a piston in place of the plunger. Both dope delivery systems are satisfactory. The fiber is formed at the base of the spinnerette tip, pulled by the force of gravity. The fiber is dramatically attenuated during spinning. The fiber diameter depends on the properties of the dope, the tip diameter, and the drying conditions. The linear velocity of the fiber during spinning is 3-5 meters per second.

The first modification was to the drying gas inlet system. As the gas flow rate increased, the drying fiber began to sway excessively. The inlet system was rebuilt to incorporate a polypropylene separation tube extending 15 cm beneath the spinnerette. Surrounding the tube is a polypropylene chamber which directs the incoming drying gas so it is concentric and laminar. This suppressed the swaying problem.

The original drying gas heating system employed a heat exchanger consisting of a coil of copper tubing in a heated oil bath. This proved inadequate, and attempts to increase heat transfer by packing the tube with steel wool made no improvement. It became clear that both the gas

temperature and mass flow rate had to be significantly increased. The oil bath system was scrapped and replaced with a hot air blower using a laboratory heat gun as the air heater. The drying gas inlet system was rebuilt using glass and copper to withstand higher temperatures and larger inlets to accommodate the higher mass flow rate. We believe this system provides enough heat and mass flow. Unfortunately, the fiber at the exit, while dry enough to retain its shape, is still too tacky to be directly spooled.

The major problem with the apparatus is the inadequate length of the drying column, which is presently restricted by ceiling height. The residence time for the drying fiber is only a few tenths of a second. The fiber cannot be directly collected on the spooler at this time. Instead we are collecting the fiber by draping it over a rod which is oscillated across the path of the partially dried fiber at the exit of the column. The fibers dry completely in a few seconds on the rod. With care to prevent the tacky fibers from tangling, it is possible to recover lengths of about 10 meters of unbroken fiber. This is adequate for present needs in sintering and textural studies. Truly continuous spinning will require a much longer drying system. In the short run we will have continuous fibers spun at Albany International Research Company, which is providing consulting services for fiber spinning. In their facilities we can also spin multifilament fibers instead of monofilaments.

Disposable tapered tip spinnerettes were used in the present experiments. The specifications of the spinnerette used in the earlier work was 22 Gauge (410 microns) and 33 mm long. The actual diameter was 460 microns. These spinnerettes gave a maximum dry fiber diameter of 40

microns (the conditions will be discussed in the succeeding section). In order to increase stiffness of the dry fiber, an attempt was made to increase the diameter of the spinnerette by cutting the tapered tip. This increased the diameter, but decreased the length. Since the spinning dope is viscoelastic, it has memory effects. The diameter ( $d$ ) of the spinnerette is as important as the length ( $l$ ), since the ( $l/d$ ) ratio determines the die swell phenomenon at the spinnerette. Minimal die swell is essential for uniform fiber spinning. Keeping this in mind, three spinnerettes with the same length of 33 mm, but diameters of 1200, 840, and 580 microns were used to examine the effect of diameter.

Using the standard formulation 24424-1, experiments were done at various spinning conditions including the air pressure to the dope delivery system (which determines the extrusion rate), the temperature of the oil bath in the earlier set up, the mass flow rate of the drying gas (as controlled by the nitrogen pressure), the length of the drying column (by number of sleeves), and the  $l/d$  ratio. The criterion for acceptable extrusion rate for the dope delivery system was that for a given spinnerette  $l/d$  ratio, the flow was smooth, and the die swell was minimum in the absence of the drying gas. Subsequently, the drying gas was introduced at a flow rate such that it would not create major turbulence on the fiber.

The spinning conditions and the corresponding fiber diameters at different  $l/d$  ratios are summarized in Table 5.3. The experiments using a 460 micron spinnerette with a  $l/d$  ratio of 717 showed some dependence of the fiber diameter on the air pressure to dope delivery as well as the drying gas pressure (nitrogen at 30°C). The fiber spun at 15 psi air and 5

psi N<sub>2</sub> pressure resulted in fibers about 30 micron diameter as shown in Figure 5.5A. The fibers spun at these conditions produced long lengths of fibers and formed the starting point for further study.

Experiments were carried out using the 22 gauge spinnerettes to different diameters and lengths (thereby altering the l/d ratios). Using a 700 micron diameter spinnerette with an l/d ratio of 443, the experiments showed the sensitivity of the dry fiber diameter to extrusion rate and drying conditions, as determined by air and N<sub>2</sub> pressures. The fibers produced at 10psi air and 10 psi N<sub>2</sub> produced 56 micron fibers (Figure 5.5B) whereas the fibers produced at 10 psi air and 20 psi N<sub>2</sub> has a diameter of 80 microns as shown in Figure 5.5C. In both cases the fibers were uniform in shape and in binder distribution. The Table 5.3 indicates that the maximum diameter that can be spun is approximately 1/10 the diameter of the spinnerettes (these experiments were done using the cut spinnerettes). This will be further examined by the spinnerettes of the same lengths as the last experiment (at 1000 micron dia cut spinnerette) showed some die swell due to the smaller l/d ratio.

#### 5.4 Viscoelastic Investigation of the Spinnability of the Dope

The spinnability of the dope depends both on viscosity and surface tension of the fluid<sup>11</sup>. Our spinning dopes, measured on a Haake rotational viscometer, have a viscosity range of 6000-7000 cps at a shear rate of 0.1 reciprocal seconds, which is considered appropriate for a solution spinning

---

<sup>11</sup> "Formation of Synthetic Fibers", Z.K. Walczak, Gordon & Breach Science Publishers, NY 1977

Table 5.3  
Fiber Diameter At Different Spinning Conditions

<u>EXPT NO</u>	<u>Spinnerette Dia (microns)</u>	<u>L/D</u>	<u>Air Pressure (psi)<sup>a</sup></u>	<u>N<sub>2</sub> Pressure (psi)<sup>b</sup></u>	<u>Fiber Dia (micron)</u>
B5-71	460	717	15	5	30
B22-72	700	442	5	10	38
B24-72	700	442	5	10	56
B25-72	700	442	10	20	85
25187-2A	700	442	10	20	80
25187-2B	1200 <sup>c</sup>	241	15	20	39
25187-2C	1200	241	10	20	52
25196-B2	1200	241	15	25	68
25196-B3	1200	241	8	25	101
25196-B15	1200	2421	15	25	98

<sup>a</sup> Air pressure at the dope delivery system.

<sup>b</sup> N<sub>2</sub> pressure at the inlet of the heat exchange unit. The temperature was at the maximum 30°C irrespective of Oil bath temperature.

<sup>c</sup> Diameter was obtained by cutting the 22 gauge (460 microns, 33mm long) to different lengths to obtain L/D.



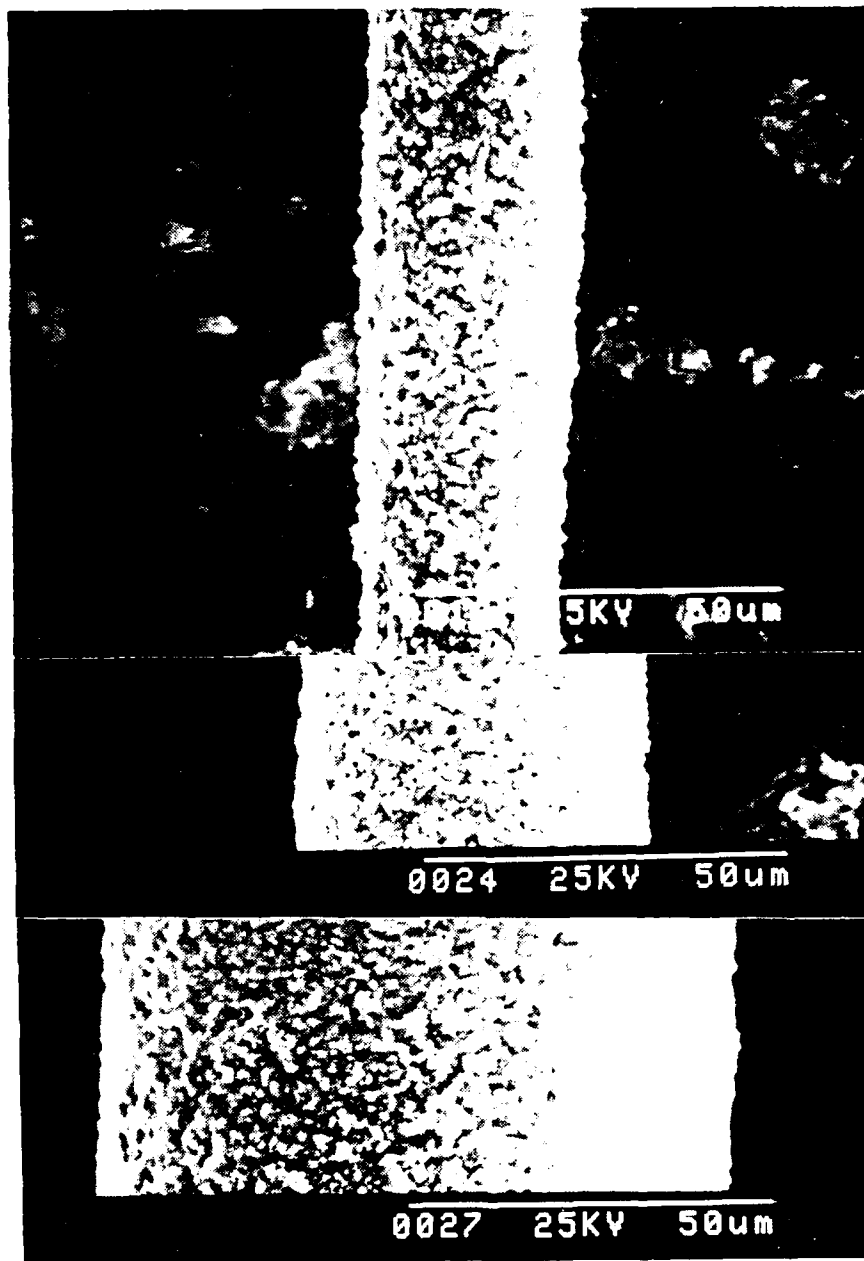


Figure 1 Barium Titanate Green Fibers at Various Spinning Conditions. See Text

process. We sought to employ the "Dynamic Mechanical Spectra" technique to characterize the viscoelastic properties<sup>12</sup> of the spinning dope.

Since the spinning dope consists of amorphous polymers in solution, it was important for us to investigate whether the adsorbed polymer layer could act as the entanglement link or real physical entanglements were necessary to form the fibers. In the absence of crystallinity, only entanglements of the polymer could result in fiber formation in either case. Also it is important to characterize the spinning dope itself to establish a "viscoelastic fingerprints" of the spinnable dope. The idea was to compare any new formulation or preparation procedure of the spinning dope by the same procedure.

#### 5.4.1 Dynamic Mechanical Analysis

Dynamic Mechanical analysis probes into the viscoelastic response of polymeric materials. The experiment is schematically shown in Figure 5.6. A sinusoidal stress or strain (within the linear viscoelastic regime) is applied to the sample either in tension or in shear to a sample of appropriate geometry. The corresponding strain or stress, which will be out of phase with the forcing function, is monitored to characterize the viscoelastic response of the material. The tangent of the phase lag (Tan Delta) is the ratio of the loss modulus  $G''$  to the storage modulus  $G'$  per cycle of the experiment (in shear for example). The quantities  $G'$  and  $G''$  are related to the complex viscosity,  $\eta^*$ , of the material.

---

<sup>12</sup> "Physical Properties of Polymers" A. Graessley in Chapter 3, page 97, American Chemical Society, Washington DC 1984.

The measured quantities in the experiment are the phase lag, and the amplitude of the response function. The quantities  $G'$ ,  $G''$  and  $n$  plotted as a function of the measurement frequency constitute the viscoelastic spectrum at a given temperature (example of a polymer melt is shown in Figure 5.6). Measurements are usually done over a frequency of 0.01 Hz to 100 Hz.

#### 5.4.2 Measurements on Spinning Dope

Dynamic mechanical measurements were carried out on the spinning dopes to establish the "Viscoelastic Fingerprint" of the present spinnable formulation. Measurements were also carried out as a function of solids loading to understand the 'Spinnability' of the material. Subtle changes in formulation, and sample milling time were examined.

Experiments were carried out on the Rheometrics Dynamic Mechanical Analyzer at the University of Lowell. The frequency range was 0.01 Hz to 100 Hz at ambient conditions. A 5% strain level was chosen for all the measurements (well within the linear viscoelastic range for a liquid).

The data for the standard barium titanate formulation 24424-1, mixed for 18 hrs is shown in Figure 5.7. Both  $G'$  and  $G''$  increase with frequency whereas  $n$  decreases due to shear rate effects. The cross-over where  $G''$  is greater than  $G'$  occurs much below 1 Hz and extends to 100 Hz. This regime is indicative of the rubbery plateau of the material, i.e., physical entanglements of the polymeric species in the dope. This formulation has appropriate viscosity for good fibers in the spinning experiment.

Longer milling (36 hrs) caused a different viscoelastic spectrum. Figure 5.8, in terms of the magnitude and cross-over of  $G'$  and  $G''$  in the

frequency domain. Also the viscosity at low frequencies is higher. The loss modulus  $G''$  becomes greater than the storage modulus  $G'$  once again at 10 Hz indicative of the glassy phase. This sample, though spinnable, was viscous to handle. Additional mechanical mixing may have triggered partial cross-linking reaction of the Cymel 370 with QR-1074 resin, and hence an increase in viscosity.

Experiments were carried out on the neat resin (i.e. 24424-1 without the barium titanate powder), and at different powder levels 25%, 50% and 75% of the total powder level of the formulation 24424-1. The neat resin spectrum in Figure 5.9 shows no crossover in the frequency range and the loss modulus  $G''$  is larger than the storage modulus  $G'$ , which is indicative of flow behavior. The condition  $G' > G''$  will be at frequencies higher than 100 Hz indicating a short entanglement relaxation time. This neat resin composition was not fiber-forming.

Similar results were found for dopes of 25 wt% and 50 wt% powder levels. At 75 wt% powder level the cross-over  $G' > G''$  occurs at 0.5 Hz, and ends before 2 Hz. The entanglement relaxation time is shorter and the distribution is very narrow compared to the standard formulation 24424-1. This material was a poor fiber former by spinning experiments.

The above studies have indicated that an appropriate viscosity coupled with the entanglement relaxation time ( $G' > G''$ ) is crucial in fiber formation from the spinning dope. The formulation 24424-1 has the appropriate powder content for fiber formation. At this level of powder, the polymers that showed no entanglements in neat resin, show a rubbery plateau throughout the regime. It appears that the viscoelastic response is a good indicator of the spinnability of the dope.

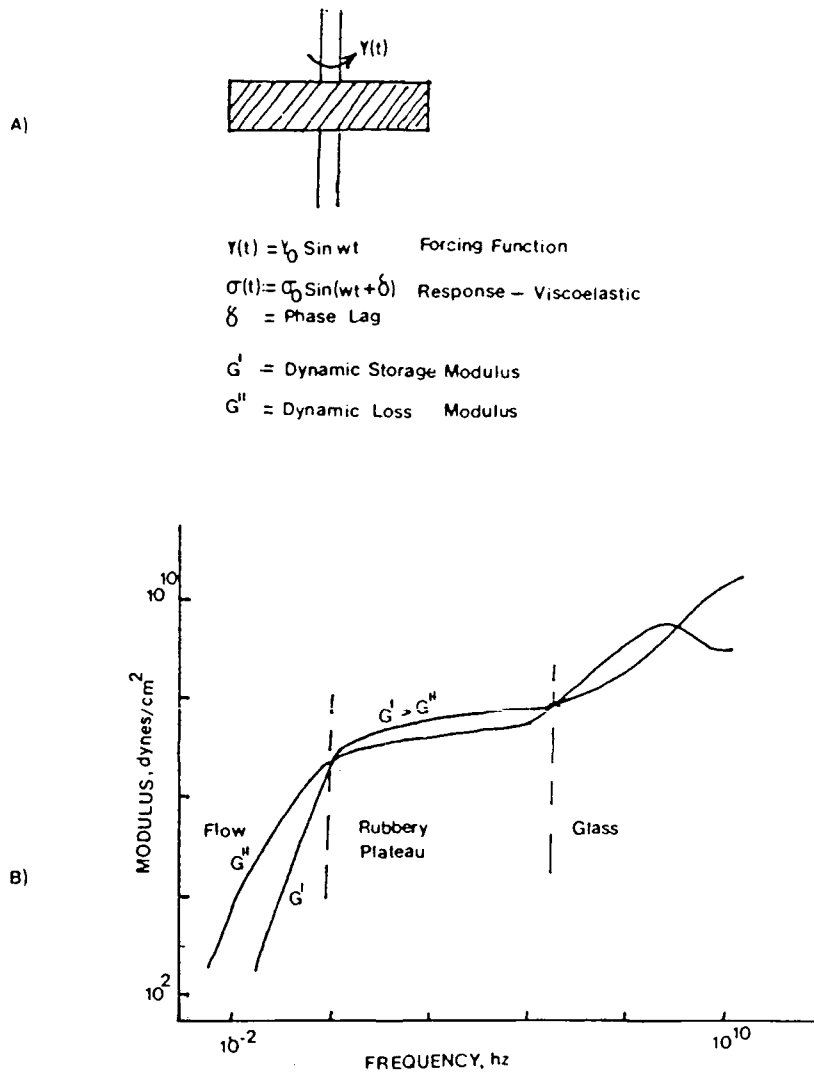


Figure 5.6

- A) Dynamic Mechanical Analysis Experiment
- B) Viscoelastic Response of a Typical Polymer Melt Showing Flow Region at Low Frequencies, where Loss Modulus  $G''$  exceeds Storage Modulus  $G'$ , Rubbery Plateau at Intermediate Frequencies, and Glass Region at High Frequencies

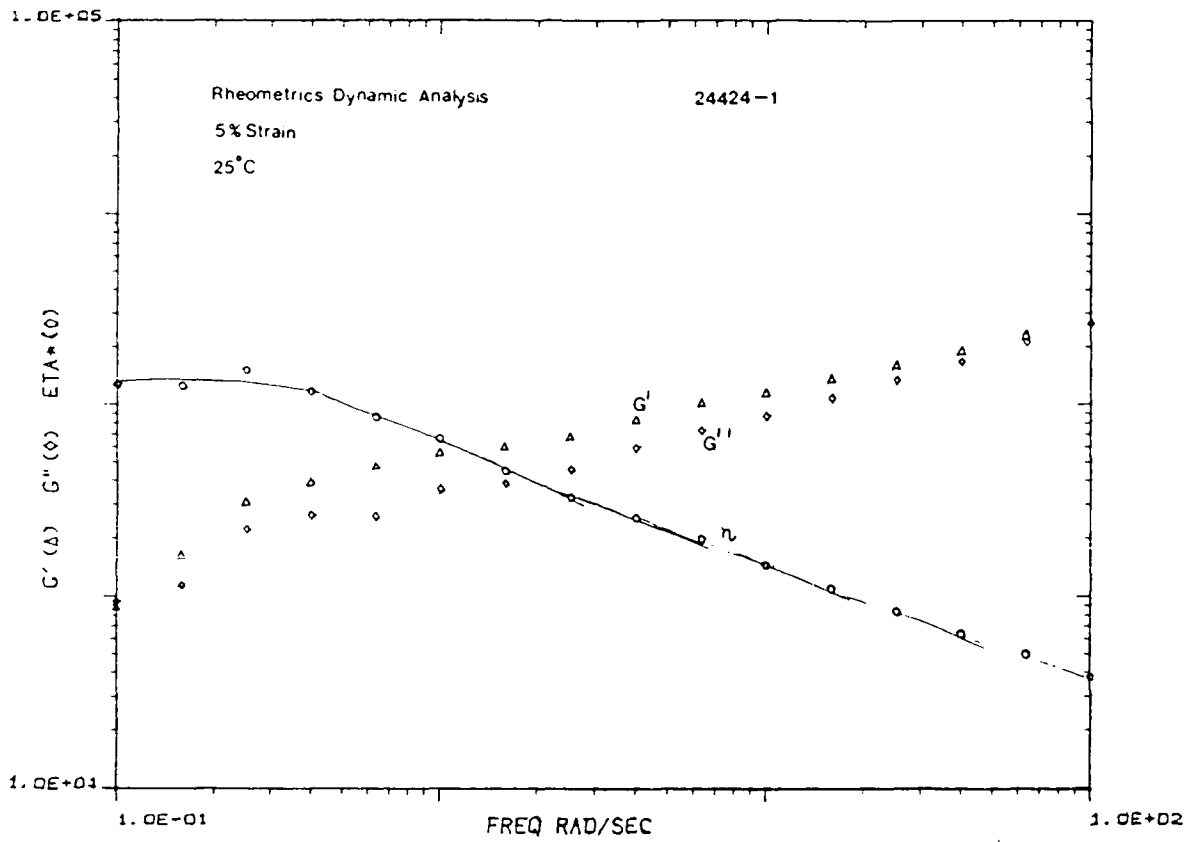


Figure 5.7 Viscoelastic Response of Standard Spinning Dope Formulation 24424-1 Milled 18 hours

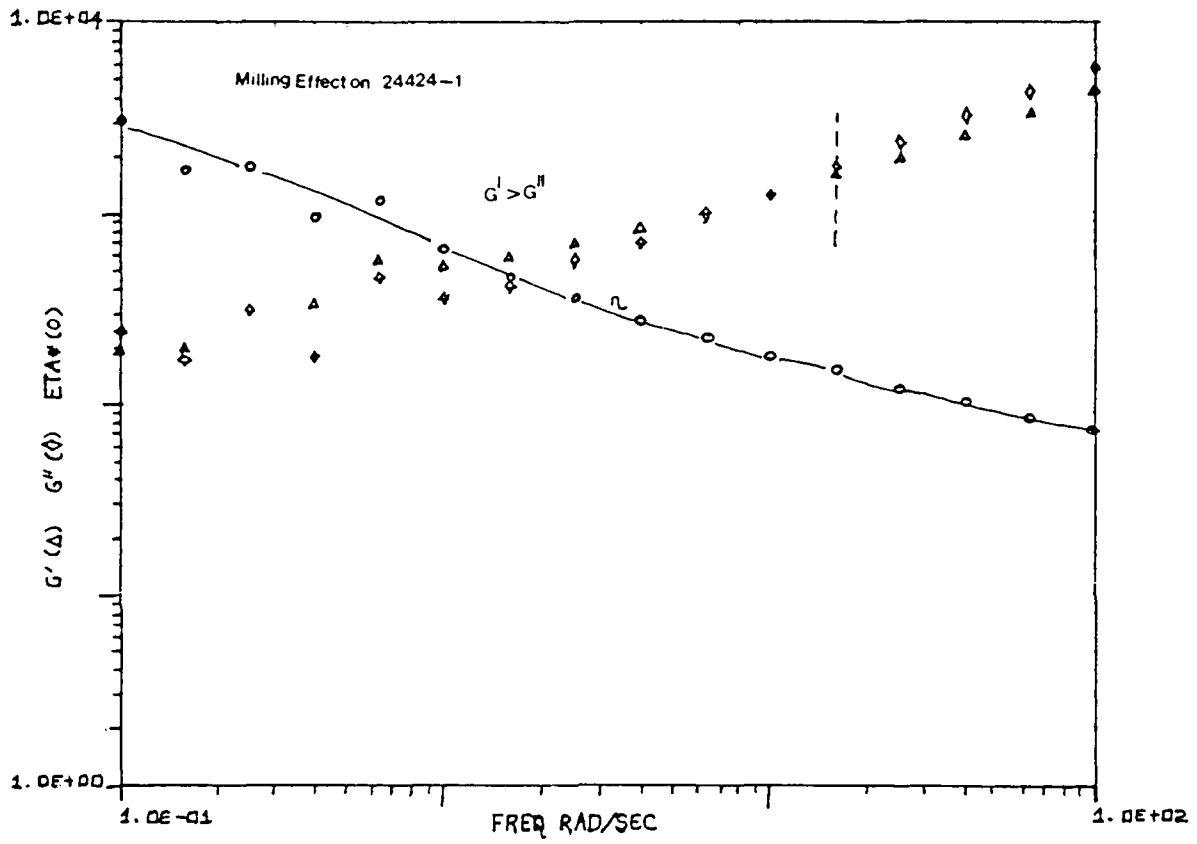


Figure 5.8 Viscoelastic Response of Standard Spinning Dope Formulation 24424-1 Milled 36 hours

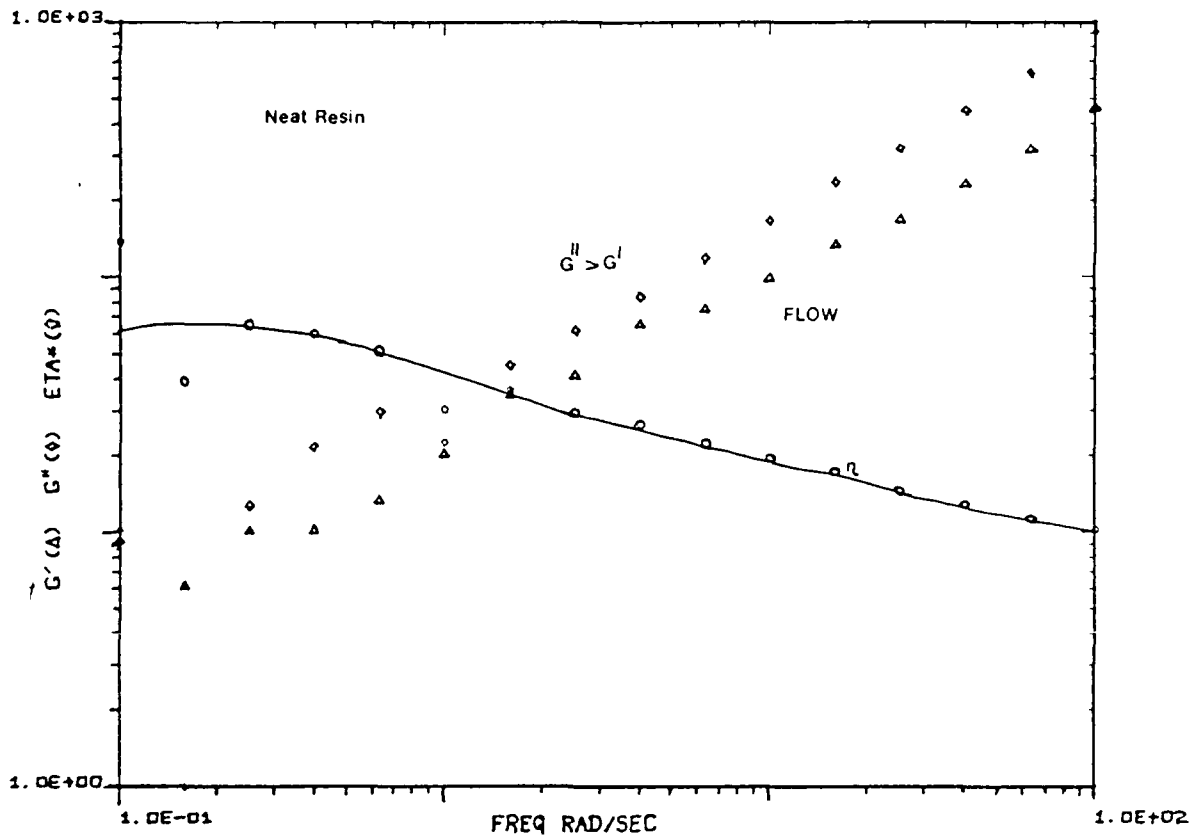


Figure 5.9 Viscoelastic Response of Spinning Dope Mixture without Powder Showing Neat Resin Behavior



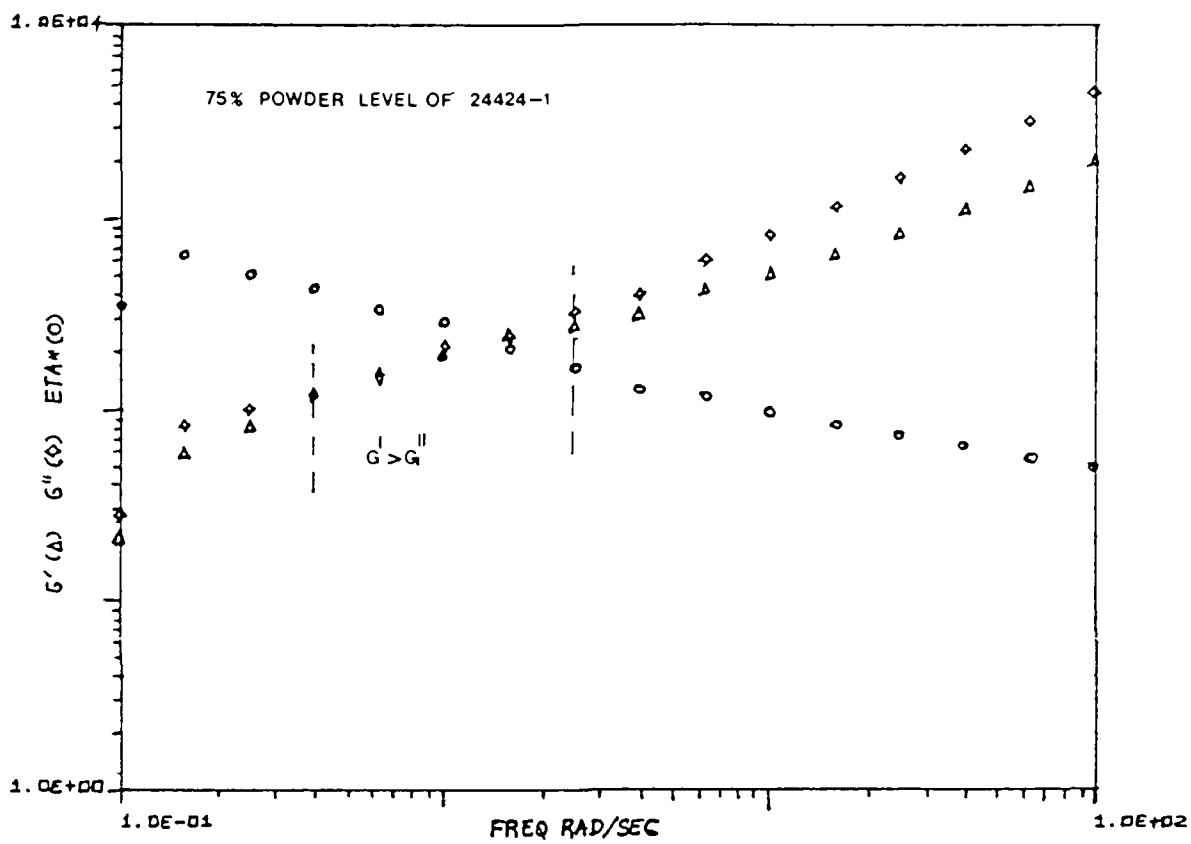


Figure 5.10 Viscoelastic Response of Spinning Dope Formulated with only 75% of Standard Powder Loading

SECTION 6  
METAL CLADDING

Cladding research received little attention during this report period, as emphasis was placed on the fabrication and sintering of  $\text{YBa}_2\text{Cu}_3\text{O}_{7-x}$  fibers. Discussions and planning continued for both the electroplating approach and mechanical cladding concept. A literature search is underway on molten salt electrolytes and non-aqueous media, and we have contacted a consultant in non-aqueous plating media. As preliminary research for molten salt electroplating, a series of screening experiments are underway to assess the compatibility of several molten salt mixtures with densely sintered  $\text{YBa}_2\text{Cu}_3\text{O}_{7-x}$  pellets. Early results are encouraging, since we have found conditions under which the pellets are not aggressively attacked. These results will appear in the next report.

## SECTION 7

## SUMMARY AND CONCLUSIONS

The sintering and microstructure development of  $\text{YBa}_2\text{Cu}_3\text{O}_{7-x}$  has been characterized for as-calcined and milled powder, both as undoped and doped with 5wt%  $\text{CuO}$ . The undoped powder reaches 94% density, with fully recrystallized grains after 15 hours at  $995^\circ\text{C}$ . The  $\text{CuO}$ -doped material sinters to full density at temperatures as low as  $925^\circ\text{C}$ , with extensive recrystallization. The resistivity has been measured as a function of temperature for nearly dense and relatively porous undoped material.

Fibers, produced by dry spinning  $\text{YBa}_2\text{Cu}_3\text{O}_{7-x}$ , can be nearly fully densified by a rapid zone sintering process. Total dwell time at peak temperature of 4-10 minutes is sufficient to densify both undoped and  $\text{CuO}$ -doped fibers. This indicates that continuous sintering of green fibers at a practical rate is feasible. After an oxygen intercalation anneal, the sintered fibers are superconducting.

The zone sintering is used to attempt to develop microstructural texture by directional recrystallization. Early results indicate the  $\langle 010 \rangle$  particle axes seem to align at 45 degrees to the fiber axis, rather than colinear with the fiber axis. This method, and other texturing methods are being further developed.

Usable fibers are being dry spun in about one meter lengths. With the current apparatus, the fibers are in fact spun continuously, but can only be collected in short lengths due to inadequate drying. The collected fiber, however, is adequate in quality and quantity for present experimental purposes. The spinnability of the dry spinning dope has been related to the viscoelastic behavior, as determined by dynamic mechanical analysis.

ATTACHMENT I

REPORT SUMMARY

COMPOSITE CERAMIC SUPERCONDUCTING  
FILAMENTS FOR SUPERCONDUCTING CABLE

Second Quarterly Interim Progress Report on  
Contract Number N00014-87-C-0780

5 January 1988

J. W. Halloran, et al., Ceramics Process Systems Corporation,  
Cambridge, MA 02139

This is the second progress report of a five month program to demonstrate the feasibility of manufacturing superconducting wires from  $\text{YBa}_2\text{Cu}_3\text{O}_{7-x}$ , consisting of a small ceramic core with a copper cladding. The ceramic core is to be produced from a dry spun ceramic fiber, sintered to create a  $\langle 010 \rangle$  fiber texture to enhance critical current. The sintered fiber is to be clad with copper by electroplating.

The sintering and microstructure development of  $\text{YBa}_2\text{Cu}_3\text{O}_{7-x}$  has been characterized for as-calcined and milled powder, both as undoped and doped with 5wt% CuO. The undoped powder reaches 94% density, with fully recrystallized grains after 15 hours at 995°C. The CuO-doped material sinters to full density at temperatures as low as 925°C, with extensive recrystallization. The resistivity has been measured as a function of temperature for nearly dense and relatively porous undoped material.

Fibers, produced by dry spinning  $\text{YBa}_2\text{Cu}_3\text{O}_{7-x}$ , can be nearly fully densified by a rapid zone sintering process. Total dwell time at peak temperature of 4-10 minutes is sufficient to densify both undoped and CuO-doped fibers. Continuous fiber sintering appears to be practical using a scaled-up version of the zone sintering process. After an oxygen intercalation anneal, the sintered fibers are superconducting.

The zone sintering is used to attempt to develop microstructural texture by directional recrystallization. Early results indicate the  $\langle 010 \rangle$  particle axes seem to align at 45 degrees to the fiber axis, rather than colinear with the fiber axis. This method, and other texturing methods are being further developed.

Usable fibers are being dry spun in about one meter lengths. With the current apparatus, the fibers are in fact spun continuously, but can only be collected in short lengths due to inadequate drying. The collected fiber, however, is adequate in quality and quantity for present experimental purposes. The spinnability of the dry spinning dope has been related to the viscoelastic behavior, as determined by dynamic mechanical analysis.

ATTACHMENT II

ARPA ORDER NUMBER: 6214

PROGRAM CODE NUMBER: 7Y10

CONTRACTOR: Ceramic Process Systems Corporation  
840 Memorial Drive  
Cambridge, MA 02139

CONTRACT NUMBER: N00014-87-C-0789

CONTRACT EFFECTIVE DATE: 8/16/87

CONTRACT EXPIRATION DATE: 1/15/88

SHORT TITLE OF WORK: Ceramic Superconductor Filaments

PRINCIPAL INVESTIGATOR: John W. Halloran  
(617) 354-2020

during the reporting period 16 October through 15 December 1987, the major progress was the production of superconductor fibers which could be rapidly sintered. The sintering and microstructure development of  $\text{YBa}_2\text{Cu}_3\text{O}_{7-x}$  has been characterized for as-calcined and milled powder, both as undoped and doped with 5wt%  $\text{CuO}$ . The undoped powder reaches 94% density, with fully recrystallized grains after 15 hours at  $995^\circ\text{C}$ . The  $\text{CuO}$ -doped material sinters to full density at temperatures as low as  $925^\circ\text{C}$ , with extensive recrystallization. The resistivity has been measured as a function of temperature for nearly dense and relatively porous undoped material.

Fibers, produced by dry spinning  $\text{YBa}_2\text{Cu}_3\text{O}_{7-x}$ , can be nearly fully densified by a rapid zone sintering process. Total dwell time at peak temperature of 4-10 minutes is sufficient to densify both undoped and  $\text{CuO}$ -doped fibers. Continuous fiber sintering appears to be practical using a scaled-up version of the zone sintering process. After an oxygen intercalation anneal, the sintered fibers are superconducting.

The zone sintering is used to attempt to develop microstructural texture by directional recrystallization. Early results indicate the  $\langle 010 \rangle$  particle axes seem to align at 45 degrees to the fiber axis, rather than colinear with the fiber axis. This method, and other texturing methods are being further developed.

Usable fibers are being dry spun in about one meter lengths. With the current apparatus, the fibers are in fact spun continuously, but can only be collected in short lengths due to inadequate drying. The collected fiber, however, is adequate in quality and quantity for present experimental purposes. The spinnability of the dry spinning dope has been related to the viscoelastic behavior, as determined by dynamic mechanical analysis.

ATTACHMENT III

ARPA ORDER NUMBER: 6214

PROGRAM CODE NUMBER: 7Y10

CONTRACTOR: Ceramic Process Systems Corporation  
840 Memorial Drive  
Cambridge, MA 02139

CONTRACT NUMBER: N00014-87-C-0789 CONTRACT AMOUNT: \$298,533.00

EFFECTIVE DATE OF CONTRACT: 16 August 87

EXPIRATION DATE OF CONTRACT: 15 January 88

PRINCIPAL INVESTIGATOR: John W. Halloran

TELEPHONE NUMBER: (617) 354-2020

SHORT TITLE OF WORK: Ceramic Superconductor Fibers

REPORTING PERIOD: 16 October 87 through 15 December 87

DISCRIPTION OF PROGRESS

During the reporting period the major progress was the production of superconducting fibers that could be rapidly sintered. The sintering and densification characteristics of  $\text{YBa}_2\text{Cu}_3\text{O}_{7-x}$  has been characterized for both undoped powder, both as undoped and doped with 5wt. CuO. The sintering process is characterized by density, with fully recrystallized grains after sintering at 925°C. The CuO-doped material sinters to full density at temperatures as low as 925°C, with extensive recrystallization. The densification has been measured as a function of temperature for nearly dense and relatively porous, undoped material.

Fibers, produced by dry spinning  $\text{YBa}_2\text{Cu}_3\text{O}_{7-x}$ , can be nearly fully densified by a rapid zone sintering process. Total dwell time at peak temperature of 4-10 minutes is sufficient to densify both undoped and CuO-doped fibers. Continuous fiber sintering appears to be practical using a scaled-up version of the zone sintering process. After an oxygen intercalation anneal, the sintered fibers are superconducting.

The zone sintering is used to attempt to develop microstructural texture by directional recrystallization. Early results indicate the  $\langle 010 \rangle$  particle axes seem to align at 45 degrees to the fiber axis, rather than colinear with the fiber axis. This method, and other texturing methods are being further developed.

Usable fibers are being dry spun in about one meter lengths. With the current apparatus, the fibers are in fact spun continuously, but can only be collected in short lengths due to inadequate drying. The

collected fiber, however, is adequate in quality and quantity for present experimental purposes. The spinnability of the dry spinning dope has been related to the viscoelastic behavior, as determined by dynamic mechanical analysis.

Feasibility of each of the process step should be demonstrated by the end of the contract period.

SUMMARY OF SUBSTANTIVE INFORMATION DERIVED FROM SPECIAL EVENTS

Project members attended the Materials Research Society Meeting in Boston, where numerous papers and posters were presented on high temperature superconductors. The information is too voluminous to summarize here.

CHANGE IN KEY PERSONNEL

No change

PROBLEMS ENCOUNTERED AND/OR ANTICIPATED

We anticipate demonstrating the feasibility of each element in the program, as outlined in the Objectives.

ACTION REQUIRED BY THE GOVERNMENT

No action is required.

FISCAL STATUS

1) <u>Amount currently received on contract:</u> (No funds have yet been received on this contract)	\$ 0.00
2) <u>Expenditures and Commitments to date:</u> (As of 12/31/87, \$223,355.00 has been expended)	\$ 223,355.00
3) <u>Funds required to complete work:</u>	\$ 298,533.00



END

DATE

FILMED

DTIC

4/88